Metabolomics characterizes early metabolic changes and markers of tolerant *Eucalyptus* ssp. clones against drought stress

Clarice Noleto-Dias[a,b,§], Edgard A. de T. Picoli[c], Andrea Porzel[b], Ludger A. Wessjohann[b*], Josean F. Tavares[a], Mohamed A. Farag[d*]

[a] Natural and Synthetic Bioactive Products Graduate Program, Federal University of Paraíba, João Pessoa, PB, 58051-900, Brazil

[b] Department of Bioorganic Chemistry, Leibniz Institute of Plant Biochemistry, Halle (Saale), 06120, Germany

[c] Plant Biology Department, Federal University of Viçosa, Viçosa, MG, 36570-900, Brazil

[d] Pharmacognosy Department, College of Pharmacy, Cairo University, Cairo, 11562, Egypt

[§] Present address: Plant Sciences and the Bioeconomy, Rothamsted Research, West Common, Harpenden, Hertfordshire AL5 2JQ, UK.

[*] Corresponding authors' email: mohamed.farag@pharma.cu.edu.eg, ludger.wessjohann@ipb-halle.de

Abstract

Eucalyptus L'Hér. (Myrtaceae) is one of the economically most important and widely cultivated trees for wood crop purposes worldwide. Climatic changes together with the constant need to expand plantations to areas that do not always provide optimal conditions for plant growth highlight the need to assess the impact of abiotic stresses on eucalypt trees. We aimed to unveil the drought effect on the leaf metabolome of commercial clones with differential phenotypic response to this stress. For this, seedlings of 13 clones were grown at well-watered (WW) and water-deficit (WD) conditions and their leaf extracts were subjected to comparative analysis using ultra-high performance liquid chromatography coupled to mass spectrometry (UPLC-MS) and nuclear magnetic resonance spectroscopy (NMR). UPLC-MS and NMR analyses led to the annotation of over 100 molecular features of classes such as cyclitols, phenolics, flavonoids, formylated phloroglucinol compounds (FPCs) and fatty acids. Multivariate data analysis was employed for specimens' classifications and markers identification from both platforms. The results obtained in this work allowed us to classify clones differing in drought tolerance. Classification models were validated using an extra subset of samples. Tolerant plants exposed to water deficit accumulated arginine, gallic acid derivatives, caffeic acid and tannins at higher levels. In contrast, stressed drought-sensitive clones were characterised by a significant reduction in glucose, inositol and shikimic acid levels. These changes in contrasting drought response eucalypt pave ways for differential outcomes of tolerant and susceptible phenotypes. Under optimal growth conditions, all clones were rich in FPCs. These results can be used for early screening of tolerant clones and to improve our understanding of the role of these biomarkers in *Eucalyptus* tolerance to drought stress.

KEYWORDS: *Eucalyptus*, Myrtaceae, UPLC-MS, NMR, phenolics, flavonoids, formylated phloroglucinols, water deficit.

1. Introduction

Eucalyptus L'Hér. (Myrtaceae) is one of the economically most important hardwood crops worldwide. They are widely cultivated in as many as 95 countries owing to their high-yielding forests (Zhang and Wang, 2021). Brazil is a global leader of forest productivity. In 2021, *ca*. 9.3 million hectares of trees were planted for industry purposes in Brazil, with cultivated *Eucalyptus* to account for the larger portion of this area (80.2%). Most plantations are based on clonal material of *E. grandis*, *E. urophylla* and their hybrids (IBGE, 2021).

Due to its exceptional wood quality, eucalypt biomass is a common source for timber, bioenergy, and pulp for paper production (Oberschelp et al., 2022). Therefore, eucalypt plantations contribute to decreasing the exploitation of tropical forests and associated biodiversity, providing pulpwood, charcoal, and firewood as well as solid wood products (Cook et al., 2016).

Climatic changes together with the constant need to extend plantations to marginal areas that do not always provide optimal conditions for plant growth highlight the need to assess the impact of biotic and abiotic stresses on eucalypt trees (Correia et al., 2018). Stress inhibits the normal functioning of the plant and impair its growth. Consequently, these are the main problems affecting agriculture, and reduction in crop yield causes important economic losses (Mahajan et al., 2005). Future scenarios indicate low precipitation levels and more frequent droughts in tropical regions such as most part of Brazil. Water deficit has significant detrimental impact on plant metabolism and productivity (Florêncio et al., 2022). In eucalypts, water deficit can intensify a physiological disorder called dieback that leads to dried twig tips that can rapidly evolve to defoliation and the death of the shoot apex (Condé et al., 2020).

Plants exposed to adverse conditions can overcome such stress *via* the excessive production of reactive oxygen species (ROS) as a defence response by activating different antioxidant mechanisms (Gill and Tuteja, 2010). One of these mechanisms involves the biosynthesis of phenolics, acting as ROS scavengers. Such plasticity of plant secondary metabolism provides a basis for the evolution of plant adaptation to changing environmental conditions (Farag et al., 2009). The knowledge gained from its upregulation can be used for future metabolic engineering attempts in the development of drought tolerant plants (Tomé et al., 2021). Consequently, understanding the metabolite variations in plants grown under water deficit is indeed a noteworthy strategy to identify biomarkers associated with stress tolerance in crop plants (Talhaoui et al., 2015).

Previously we have shown that drought tolerant *Eucalyptus* seedlings upon exposure to drought stress yielded higher quantities of phenolics in their leaves than their sensitive counterparts at the same conditions (Dias et al., 2017). Untargeted metabolomics is a potential approach to monitor and link specific variations by analysing diverse metabolite classes. A comprehensive view of the metabolome at a certain environmental condition unable the identification of trait specific chemical markers that can

be used as adaptability predictors in breeding programs. Such unbiased and holistic analysis provide a broad insight of the biochemical composition of a plant system and differences/similarities between tested groups can then be used as a diagnostic tool for plant performance. Findings can then be used in prediction models to assist breeders in the early detection of stress resistant specimens (Tomé et al., 2021; Villate et al., 2021).

Plants encompass different classes of metabolites, with varied physicochemical properties. Considering this complexity, analytical platforms applied in metabolomics studies typically target the detection of the largest number of metabolites in the envisaged metabolome (Farag et al., 2022). The ideal protocol evolves the complementarity of more than one type of analytical technique (Bijttebier et al., 2016). In this context, ultra-high performance liquid chromatography coupled to mass spectrometry (UPLC-MS) and nuclear magnetic resonance spectroscopy (NMR) complement each other with regards to metabolite coverage and level and structural elucidation, providing detection of a wide-range of metabolites (Serag et al., 2023). UPLC-MS is one of the most sensitive methods allowing for the detection of a broad range of compounds, such as phenolic acids, flavonoids, alkaloids, phenylpropanoids and others. Nonetheless, ESI-MS measurements fail to detect primary metabolites in addition to its less powerful structural elucidation power which can be overcome with NMR analysis, which is highly quantitative and robust, though less sensitive than MS (Gromski et al., 2015).

To further enhance our understanding of eucalypt drought adaptation in their early growth stages, we performed a water deficit experiment using seedlings of 13 commercial clones of *Eucalyptus* spp. with differential phenotypic response to drought. We aimed to unveil the drought effect on the leaf metabolome of these clones to assess metabolic reprograming that can be used for early selection of clones with enhanced tolerance. Clone's metabolite responses are the most determinant of plant phenotype and can provide insights on plant capacity to tolerate drought stress and aid future biotechnological attempts to engineer improved resistant accessions.

2. Results and Discussion

The major goal of this study was to investigate the effect of water deficit on *Eucalyptus* secondary metabolites in an untargeted, holistic manner in the context of their genetic diversity (distinct species/hybrids) and capacity to tolerate drought conditions (sensitive and tolerant). These results are useful for creating more efficient, accessible, and less time-consuming approaches in the screening of eucalypt clones more tolerant to water deficit.

The adopted approach is focused on developing fast and effective analytical methods for metabolomic studies of eucalypt leaves by direct extract analyses using UPLC-MS in parallel with ^{1}H-NMR. Owing to the complexity of the acquired spectral data, statistical multivariate analyses, e.g. PCA and OPLS-DA were performed to ensure good analytical rigorousness and define both similarities and differences among samples.

Initial visualization of the UPLC-MS and NMR data showed that different lines and treatments were qualitatively similar. Variability was mostly due to differences in metabolite concentrations in the

extracts. Therefore, to simplify metabolite profiling results, we prepared a pooled material from all samples and analysed its extract by both UPLC-MS and NMR. Variations among the detected molecular features were further assessed along the 13 clone lines and the different treatment conditions supported by different chemometric tools.

2.1 Leaf metabolome of eucalypt seedlings

Leaf material of eucalypt seedlings were extracted with water:methanol (50:50, v/v) and analysed *via* UPLC-MS with a reversed-phase column in negative ionization mode. Base peak chromatogram is presented in Fig. 1 with numbering used in **Table 1**. Chemical structures of identified peaks are represented in Fig. 2. Further TIC and PDA chromatograms (in 280 and 240 nm) are shown in Fig. S1. A total of 97 molecular features were identified, of which 24 were confirmed with authentics. The elution order of the compounds followed a sequence of decreasing polarity, where we can highlight the detection of cyclitols, phenolics, flavonoids, formylated phloroglucinol compounds (FPCs) and fatty acids (Fig. 1). Several of these molecular features are *O*-conjugated to sugar units and were identified based on neutral losses of 176 amu (i.e., glucuronic acid), 162 amu (hexose: i.e., glucose or galactose), 146 amu (deoxyhexose: i.e., rhamnose), and 132 amu (pentose: i.e., arabinose). So far, this is one of the most comprehensive metabolome reports for eucalypt seedlings, covering various classes of compounds and a high number of molecules. The following subsections describe the features used to identify the different metabolite classes.

2.1.1 Cyclitols

Cyclitols level found in a plant is considered an interesting trait for crop breeding. These polyols may store and transport carbon. Such properties suggest for their ability to ameliorate the effect of water deficit and protect plant cells from dehydration. Therefore, this molecular class can be a biomarker for enhanced water deficit tolerance and be monitored for supporting the adaptive strategies on agricultural crops (Çevik et al., 2014; Merchant and Richter, 2011).

Molecular features of this class were identified in *myo*-inositol (**L2**) that was confirmed with authentic standard. Quinic acid was annotated in **L3** (Fig. S2) and as conjugated to galloyl (**L9**), p-coumaroyl (**L18**, **L26**, Fig. S3), caffeoyl (**L21**, and **L33**) and feruloyl (**L30**) moieties. Shikimic acid (**L5**) and galloylshikimic acid (**L12**, Fig. S4) were tentatively identified using the results reported in literature (Tuominen et al., 2013).

Particularly, inositol is reported as a booster for the accumulation of some essential mineral elements (Amaral and Brown, 2022). It also functions as a catalyst for central enzymes to sugar metabolism, a monomer component of cell wall synthesis (Abid et al., 2009) and a player in plant tolerance to abiotic stress (Jia et al., 2019). Together with our results, these reports are aligned with the understanding of such compound being used as biomarker for water deficit tolerance in plant species and extend that to be included for eucalypt.

2.1.2 Phenolics

Marsh et al. (2017) characterised by UPLC-MS/MS the foliar polyphenol composition of 515 eucalypt species. Although the broad diversity of species, only one of the species in our study (*E. grandis*) was included in their work. Accordingly, ellagitannins were the main components in their samples and flavonol glycosides were mostly represented by quercetin 3-*O*-derivatives.

In our study, gallic (**L10**), protocatechuic (**L15**), methyl gallic (**L20**), caffeic (**L24**), *p*-coumaric (**L29**) and ellagic (**L35**) acids were confirmed with authentic. Glycosylated conjugates of these phenolic acids were also detected in eucalypt extracts. Three peaks with $[M-H]^-$ at *m/z* 483.078 were detected at 1.38 (**L11**), 2.71 (**L16**) and 4.65 (**L23**) min, indicating isomers of gallic acid dimers conjugated with hexosides. The first was tentatively identified as digalloyl-*O*-hexoside based on its MS/MS spectrum. While the two later peaks had an extra MS/MS product ion at *m/z* 439 consistent to the loss of CO_2 from a free carboxylic acid group. This suggests that one of the gallic acid units is linked *via* an ether bond between hydroxyl groups (OHs) and, therefore, these molecular features are assigned as gallic acid-galloyl *O*-hexoside isomers. Later elution time, peak **L43** with $[M-H]^-$ at *m/z* 483.187 (Fig. S5) was tentatively identified as a gallotannin conjugated to a monoterpene, globulusin A, using results reported by Hasegawa et al. (2008) that isolated this compound from *E. globulus*.

Six ellagitannins were identified in peaks **L6**, **L7**, **L17**, **L25**, **L28** and **L32**, as evident from their MS/MS product ion at *m/z* 300.9 corresponding to ellagic acid obtained from the lactonization of the hexahydroxydiphenoyl unit (HHDP). Among these, we can highlight HHDP *O*-hexoside (**L6**) and HHDP galloyl and digalloyl *O*-hexoside (**L7**, **L17** and **L25**). All these tannins have been previously reported in *Eucalyptus* leaves (Santos et al., 2013). It is worthy to mention that phenolics were successfully used in discriminating water deficit tolerant eucalypts in previous work (Dias et al., 2017).

3.1.3 Flavonoids

Flavonol was the most abundant subclass among the assigned flavonoids. The MS/MS signal of quercetin residue at *m/z* 301 ($C_{15}H_9O_7^-$) was detected in 9 peaks: **L34** (Fig. S6), **L37**, **L38**, **L39**, **L41**, **L45**, **L46** (Fig. S7), **L52** (Fig. S8) and **L56**. Myricetin 3-*O*-glucuronide (**L31**) and its aglycone (**L55**) were assigned due to their MS/MS signal at *m/z* 317, representing $[M–176–H]^-$ (loss of glucuronic acid) and $[M–H]^-$, respectively. Five kaempferol derivatives were detected in peaks **L40**, **L44**, **L47**, **L59** (Fig. S9), **L63** based on their MS/MS spectra.

Methylated flavones are commonly found in *Eucalyptus* species (Amakura et al., 2009; Hongcheng and Fujimotot, 1993). In this study, peaks **L74** and **L75** were assigned to 8-demethylsideroxylin and 8-demethyleucalyptin, respectively, based on their $[M-H]^-$ at *m/z* 297.0773 and 311.0930 and the typical losses of methyl and methoxy groups, such as the base peak of **L74** at *m/z* 282 $[M-CH_3-H]^-$ and of **L75** at *m/z* 296 $[M-CH_3-H]^-$.

2.1.4 Phloroglucinols

Peak **L67** with an [M-H]$^-$ at *m/z* 223.0979 and daughter ions *m/z* 179 [M–CO_2–H]$^-$, 167 and 153 [M–C_4H_6–H]$^-$ (Fig. S10) was tentatively identified as 2,6-dihydroxy-4-methoxy-3-methylisopropiophenone (Fig. 2), a compound previously detected in *E. pulverulenta* (Bolte et al., 1984). Robustaol B (**L69**) was identified due to its [M-H]$^-$ at *m/z* 209.0823 and fragment ions at *m/z* 194 resulting from the loss of a methyl group, as well as 166 [M–C_3H_7–H]$^-$, from the loss of the isopropyl residue (Fig. S11).

Peaks **L71** and **L77** were tentatively identified as phloroglucinol derivatives, albeit their final chemical structures were not confirmed. **L71** exhibits [M-H]$^-$ at *m/z* 237.1133 ($C_{13}H_{18}O_4$) and its MS/MS spectra (Fig. S12) indicates that this molecular feature could be both 1-(2,6-dihydroxy-4-methoxy-3,5-dimethylphenyl)-2-methyl-1-propanone and aspidinol D, compounds previously isolated in *Eucalyptus* species (Bolte et al., 1984; Cheng and Snyder, 1991). Similarly, **L77** with [M-H]$^-$ at *m/z* 251.1288 (Fig. S13) could be 4-*O*-demethyl miniatone (Sidana et al., 2012).

Diformylphloroglucinol (**L58**) was annotated based on its [M-H]$^-$ at *m/z* 181 yielding further fragment ions at 153 [M–28–H]$^-$ and 135, corresponding to the loss of an aldehyde and subsequent hydroxyl group, respectively (Fig. S14) (Chenavas et al., 2015). L68 was tentatively identified as jensenone based on its molecular feature. It presented product ions suggesting for the loss of a formyl group (*m/z* at 237), followed by subsequent loss of H_2O (*m/z* at 221), and loss of two formyl groups (*m/z* 209 – $C_{11}H_{13}O_4$), followed by the loss of H_2O (*m/z* 191 - $C_{11}H_{11}O_3$) (Fig. S15). Grandinol and homograndinol, other two monomeric FPCs, were tentatively identified in peaks **L80** and **L84**, **Table 1**.

Molecular features of dimeric FPCs were also identified in our samples. Two different dimers of grandinol (peak **L86** and **L93**, Fig. S16 & S17), jensenal (peak **L94**, Fig. S18), grandinal (a dimer of jensenone and grandinol) (peak **L96**, Fig. S19). Two types of FPCs-coupled sesquiterpenoid were characterised, a macrocarpal (peak **L91** – $C_{28}H_{40}O_6$, Fig. S20) and a euglobal (peak **L97** – $C_{23}H_{30}O_5$, Fig. S21). The chemical structure of some peaks was categorized as FPCs, based on their chromatographic and spectroscopic data, like eluting lately during the run and presenting key MS/MS product ions, *i.e.* at *m/z* 181, 193, 207, 223, 235, 237 and 249. They are described in **Table 1** as unknown FPCs (9 peaks) and terpene alcohol FPCs (**L76**, **L87**) and are potentially novel compounds. However, further work including isolation and structure characterization is needed to confirm their identification using other spectroscopic techniques.

2.1.5 Fatty acids

Eight fatty acids were characterised in the second half of the chromatographic run (13 to 23 min). Peaks **L64** and **L66** had [M-H]$^-$ at *m/z* 327 ($C_{18}H_{32}O_5$) and 329 ($C_{18}H_{34}O_5$). This extra 2 amu in the mass of **L66** indicated one double bond less in its structure. Based on their molecular formula, **L64** was tentatively identified as trihydroxy-octadecadienoic acid (Fig. S22) and **L66** 9,12,13-trihydroxy-10-octadecenoic acid (Fig. S23). **L72** encompasses one hydroxyl group less in its structure than L66; therefore, **L72** was annotated as dihydroxy-octadecenoic acid. Finally, linolenic (**L85**), linoleic (**L89**), palmitic (**L90**) and stearic (**L92**) acids were tentatively identified based on their exact masses and predicted molecular formula.

2.2 ^{1}H-NMR fingerprinting and assignments of metabolites

For visualization, ^{1}H-NMR spectrum from *E. grandis* × *urophylla* (clone Suz12) is displayed in Fig. S24 as an example of *Eucalyptus* spp. leaf extract. Three main chemical shift regions can be observed; an upfield region between 3.2 and 0.7 ppm with intense signals due to fatty acid protons; a mid-downfield region between 5.5 and 3.2 ppm with signals mostly ascribed to protons of sugar units, and a downfield region between 10.2 and 5.5 ppm with signals at much lower intensities that could be assigned to phenolics and formylated phloroglucinols. Assignments of ^{1}H- and ^{13}C-NMR signals were confirmed by comparison with spectra of authentic compounds and/or reported spectra from the literature and databases as well as by examination of 2D NMR spectra, as ^{1}H-^{1}H-COSY and TOCSY, ^{1}H-^{13}C HSQC and HMBC. **Table 2** summarizes the chemical shifts and the characteristic signals of the detected metabolites. These signals can be visualized in ^{1}H-NMR spectrum presented in Fig. S25. 2D NMR spectra are shown in Fig. S26–S30. Chemical structures are represented in Fig. 2.

Repeated methylene protons and the terminal methyl of fatty acids were promptly assigned to the signals at δ_H 1.28–1.31 and 0.89 ppm, respectively (**N1**). Other assigned peaks detected in the upfield region belonged to ω-3 fatty acid linolenic acid; two triplets at δ_H 2.80 (2H, *J*=6.0, H-11,14) and δ_H 0.97 (3H, *J*=7.5 Hz, H-18) from allylic methylene and the terminal methyl, respectively (**N2**). These peaks were confirmed by HMBC correlations of the first triplet with carbon resonances at δ_C 129.1 and 130.9 ppm from olefinic protons (δ_H 5.32-5.39).

Among signals in the mid-downfield, α-glucose (**N3**) (δ_H 5.10 d, *J*=3.7 Hz, H-1) and β-glucose (**N4**) (δ_H 4.472 *d*, *J*=7.8 Hz, H-1) are the most abundant compounds in all extracts. Hydroxy methine protons of the cyclitol *myo*-inositol (**N5**) were assigned to δ_H 3.96 (t, *J*=2.7 Hz, H-1), 3.46 (H-2), and 3.14 (t, *J*=9.2 Hz, H-4) and its detection is in accordance with UPLC-MS results. Two doublet of doublets at δ_H 2.19 and 2.70 (*J*=18.0, 5.0 Hz, H-7), with HMBC correlation with an olefinic (δ_c 138.7 ppm, C-3) and a carbonyl carbon (δ_c 170.1 ppm, C-1), were assigned to shikimic acid (**N6**). H-5 and H-6 (δ_H 3.67 and 3.99 ppm, respectively) were identified by ^{1}H-^{1}H COSY correlations and supporting its assignment and further by comparison with spectra from authentic standard. Gallic acid (**N7**) was assigned based on its singlet at δ_H 7.06 (H-3/H-7) attached to a carbon at δ_c 110.2 ppm and with HMBC correlations to δ_c 121.8 (C-2), 139.5 (C-5), 146.3 (C-4/C-6) and 170.3 (C-1).

Furthermore, in the aromatic region, 3-*O*-derivatives of kaempferol (**N8**) and quercetin (**N9**) were detected. Two doublets at δ_H 6.18 (*J*=2.0 Hz) and 6.40 (*J*=2.0 Hz) could be assigned to H-6 and H-8 of both flavonoids. The different resonances are due to ring B protons. In kaempferol derivatives, key doublets at δ_H 8.08 (*J*=8.8 Hz) and 6.90 (*J*=8.8 Hz) corresponded to H-2′/6′ and H-3′/5′, respectively. While for quercetin derivatives, H-6′ was assigned to δ_H 7.57 (*dd, J*=8.0, 2.0 Hz) and showed COSY correlations to H-5′ (δ_H 6.88 ppm). The detection of these two flavonols agreed with the UPLC-MS data, that showed them as the largest class of flavonoids detected in *Eucalyptus* leaves.

Most metabolites detected by NMR were also identified from UPLC-MS, **Table 1**. This complementary identification is an interesting aspect in the data analysis of this current study. Although NMR is much

less sensitive than UPLC-MS, a technique that allowed the identification of nearly 100 metabolites in our samples, ^{1}H-NMR fingerprinting gives absolute quantitative data. This means that the detection of a compound by NMR indicates high quantity in the samples. On the other hand, UPLC-MS data is influenced by differential ionisation and ion suppression, consequently, its values are presented as relative levels (Noleto-Dias et al., 2018).

2.3 Metabolic effect of drought in different eucalypt lines

Under this study experimental parameters, ^{1}H-NMR spectrum delivers absolute quantitative data for non-overlapping signals. Some of the metabolites described in **Table 2** were quantified in the extracts using the integration of their peaks against the internal standard (**Table 3**). Peaks of glucose, inositol, shikimic acid and arginine were distinctive with no signal overlap and large enough to be discriminated from the noise and therefore were selected for quantification. The highest level of glucose was detected in Suz2-WW at *ca*. 30 mg g^{-1} d.w and levels of inositol varied from 7.2 (Suz7-WD) to 26.1 (Suz8-WD) mg g^{-1} d.w. Shikimic acid level was highest in Suz3-WW (14 mg g^{-1} d.w.), whereas its level in drought-sensitive clones was reduced in water stressed samples compared to the non-stressed ones. Generally, levels of glucose, inositol and shikimic acid were more disturbed by water deficit in drought-sensitive clones. These are molecules usually involved in cell protection and energetic metabolic pathways. Their increased levels in *Eucalyptus* species indicates an acclimation response to an environmental stress and consequent tolerance to this factor (Oberschelp et al., 2022). Although not all tolerant clones showed higher levels of glucose, inositol and shikimic acid when under stress, the content of these metabolites was significantly reduced in stressed plants of drought-sensitive clones (**Table 3**). A study on two *E. globulus* clones differing in drought sensitivity showed a small increment of leaf soluble sugars in both clones as a response to water limitation. By contrast, this increase was more evident in the roots, particularly in the more sensitive clone. However, authors suggested that metabolic changes were not an adaptive physiological mechanism, but rather osmolyte accumulation due to low water levels (Shvaleva et al., 2006)

Several of these components are structural monomers of cell wall carbohydrates and have an osmotic role *in planta*. They have already been reported as traits that differ among eucalypt from mesic and xeric environments (Merchant et al., 2007), consequently, with potential contribution to water deficit tolerance phenotyping.

It was already reported that sugar levels in phloem sap were influenced by water supply (Sala et al., 2010), season and stand age (Battie-Laclau et al., 2014). As significant differences in sugar level was observed in leaves, it can be reasoned that leaves may act as a key element to water deficit resistance and in accordance with Duursma et al. (2011) reporting a weak relation of leaf area and the resistance trait. Both α- and β-glucose are associated with starch and cellulose pathways, respectively. Starch reserves are low under water deficit conditions, showing the significance of carbon shortage in water deficit responses (Arndt et al., 2008), with drought sensitive clones had significant decrease in photosynthetic rates under water deficit stress. Additionally, water potential as low as -4.5 MPa in

healthy eucalypt trees (Nolan et al., 2021) will demand strong and elastic cell walls in leaf cells of plants to withstand such stressful condition.

Arginine was differentially affected by stress among the different clones. This amino acid was detected at level of up to 65 mg g^{-1} d.w. (Suz3-WW) and was at higher levels in most of the stressed samples of the tolerant clones, with increments of 30–50% of the values detected in the well-watered plants (**Table 3**). Arginine is known to play a role in plant stress response. This amino acid was also more abundant in a stressed drought-tolerant sesame genotype (You et al., 2019). In another study, arginine promoted plant growth in wheat by mitigating drought stress, possibly by the induction of some responsive genes related to drought stress tolerance (Hussein et al., 2022). Arginine sprayed on drought stressed sugarcane plants improved leaf gas exchange and root antioxidative protection, features that are effective in attenuating water stress (Silveira et al., 2021). Thus, the accumulation of arginine in eucalypt stressed plants is in accordance with literature and this drought-responsive metabolite is possibly involved in the molecular mechanism of tolerance. Whether spraying of arginine in eucalypt trees could aid induce its resistance to drought stress ought to be examined in the future?

The changes in metabolites presented in **Table 3** illustrate the expected phenotypic plasticity from eucalypts (Booth, 2013; Valladares et al., 2007). At the same time, these results allow an alternative view of metabolic compounds that may function as biomarkers for water deficit tolerance as well as contribute to the understanding of the tolerant phenotype. The adjustment detected in our study amplify the context that strategies, such as osmotic adjustment (Lemcoff et al., 1994), may apply to eucalypt water deficit tolerance.

Metabolomics studies typically produce large datasets and to deeply explore metabolome differences among the 13 clones, multivariate data analysis of both UPLC-MS and NMR datasets were applied. The variance of the UPLC-MS and ^{1}H-NMR datasets of the well-watered seedlings of all clones was initially assessed in an unsupervised manner by PCA (Fig. S31). PCA is a clustering method to reduce data dimensionality, in which no knowledge of the datasets is required to evaluate the data and obtain the maximum variation among the samples (Brereton, 2003). Scores plots of both datasets showed some discrimination among samples, but with no clear separation regarding their response to drought (Fig. S31).

To better visualize the differences among tolerant and sensitive clones, these datasets were analysed using supervised partial least-squares discriminant analysis (PLS-DA), a multivariate dimensionality-reduction tool (Fig. 3). This chemometric tool optimizes separation between sample groups and emphasize the most relevant variables (Gromski et al., 2015). The scores plot obtained when clones were classified as sensitive or tolerant to drought showed clear group discrimination (Fig. 3A & 3B). Loading plot of the UPLC-MS dataset indicated that tolerant clones were enriched in gallic acid derivatives (e.g. gallic acid, gallic acid-galloyl hexoside, methyl gallic acid and HHDP digalloyl hexoside) and quercetin/kaempferol (oleuropeoyl) hexosides. In contrast, sensitive clones were discriminated by higher levels of glycoside derivatives of quercetin and kaempferol, FPCs and fatty acids (Fig. 3C). Loading plot resulting from the NMR dataset is complex but also revealing gallic acid

as a discriminant variable for tolerant clones (Fig. 3D). Clones from different genetic backgrounds were used for these analyses and suggestive for the applicability of these findings to other eucalypts and potentially be extended to other wood tree crops that produce similar secondary metabolites. It is also noteworthy to mention that these differences were detected in well-watered plants demonstrating that an initial screening can be done with seedlings growing at optimal conditions, without the need of a whole more complicated stress-induced experiment.

To understand whether the plant species/hybrid is an important feature in unsupervised line classification, individual PCA models were attempted on the matrix of UPLC-MS peak intensities of lines with similar genetic background. Clear separation between clones sensitive and tolerant to drought can be observed for *E. grandis* × *urophylla* (Fig. 4A), *E. grandis* × *pellita* (Fig. 4B) and *E. grandis* (Fig. 4C). This is an interesting result revealing that when we limit comparisons to a single hybrid/species, there are intrinsic metabolome differences that can explain their response to drought. These findings revealed the exciting potential of this approach to be used in breeding programs that produce large numbers of crossings from a specific set of plant species. This metabolomics approach could function as a tool for screening hybrids from the same species or parents in the search of tolerant specimens. An early and simple identification such as this would reduce time and costs for the selection of optimized lines.

To obtain further details on the effect of drought in tolerant and sensitive clones, OPLS-DA was performed separately on the datasets of each clone. For this, samples were classified according to the treatment conditions the plant were grown (stressed and well-watered). This approach is used to get a better definition of the statistically significant markers of stress response. The OPLS-DA of both UPLC-MS and NMR datasets of the drought tolerant clone Suz12 yielded excellent fit and predictivity (R^2Y_{cum} > 0.985 and Q^2_{cum} > 0.953) (Fig. 5A & 5B). Examination of their S-plots (Fig. 5C & 5D) revealed that gallic acid and caffeic acid were elevated in stressed plants versus FPCs e.g. grandinol in WW plants.

Similar results were observed for other tolerant lines when their UPLC-MS and NMR datasets were plotted in OPLS-DA models (Fig. S32). S-plots revealed that FPCs were enriched in well-watered samples and compared with these samples, the leaf metabolome of the drought stressed plants contain more tannins, gallic acid, chlorogenic acid and flavonoids (e.g. quercetin-3-glucuronide).

On another view, drought sensitive clones reacted in a slightly unique way when subjected to water deficit stress. OPLS-DA models (Fig. S33) indicated that the metabolome of stressed plants was mostly discriminated by the higher levels of ellagic acid derivatives (3-methyl-ellagic acid and ellagic acid pentoside), fatty acid (trihydroxy-octadecenoic acid) and flavonoids (apigenin, myricetin 3-glucuronide and quercetin derivatives). Well-watered plants in addition to the greater level of FPCs, also presented higher amount of quercetin derivatives and tannins (Fig. S33E - clone Suz3, *E. grandis* × *urophylla*) and quinic acid (Fig. S33G - clone Suz7, *E. grandis* × *pellita*).

Asides, OPLS-DA classification models from both NMR (Fig. S34) and UPLC-MS (Fig. S35) datasets were performed to demonstrate models' classification capacity based on external validation sets for PEG (polyethylene glycol) artificial induced drought effect to identify whether the built model based on water

deficit stress can predict tolerant and sensitive clones under an artificial drought stress effect. The training set consisted of the well-watered and water-deficit clones (144 samples), whereas external validation was conducted with the remaining PEG drought induced samples (72 samples), that were not used for the model's development. The R2Y and Q2Y values of the NMR OPLS model were at 0.90 and 0.81, respectively suggestive for the model robustness and consistent for fitness and prediction. In contrast, R2Y and Q2Y values of the UPLC-MS based OPLS based model were at 0.88 and 0.85, respectively. Multivariate OPLS-DA model showed high correlation of the PEG predicted clones to the active model form water drought stress from both datasets (Fig. S34A, B & S35A, B). Further, the area under the ROC curve (AUC) was considered as a validation criterion for its classification and was found to be at 0.983 and 0.985 for NMR and UPLC-MS dataset, respectively (Fig. S34C & S35C) and with low misclassification rates (0% for sensitive, 6.7% for tolerant in case of NMR dataset) (Table S1). In contrast, higher misclassification rates were observed in case of UPLC-MS especially for sensitive clones´ prediction at (19% for sensitive, 6% for tolerant) classification models (Table S2), indicating better classification models for NMR than UPLC-MS datasets.

The permutations plot aids in determining the likelihood that the present OPLS-DA model is erroneous, meaning that it only fits the training set well but fails to predict Y for new data. Here we compare the goodness of fit (R2 and Q2) of the original models to the goodness of fit of different models were the X-matrix remained unchanged while the Y-observations has been randomly permuted, for each Y variable predicted in the model, the results were given as Q2-intercepts. After 100 permutations, the R2 and Q2 intercept values for the NMR and UPLC-MS datasets were (0.363 and -0.495), and (0.182 and -0.377), respectively. The established model's robustness was shown by negative values of the Q2 intercept, indicating a low risk of overfitting and a robust model (Fig. S34D & S35D). The result confirmed that the established OPLS-DA model had noticeable fitness and predictability.

Multivariate approaches allowed the identification of more water deficit tolerance lines in ornamental (Mircea et al., 2023), medicinal (Chatara et al., 2023), and wood-tree (Corrêa et al., 2023) plants. Further, there was a significant difference in the phenolic compounds in leaves of an edible species (Olive) that was dependent upon genotype and season (Talhaoui et al., 2015).

Despite these successful reports and differences of biochemical levels, only proline (Mircea et al., 2023), morphophysiological and nutritional traits (Chatara et al., 2023; Corrêa et al., 2023) showed significant increase or differences. This highlight that the multivariate and multi-trait evaluation are useful for the identification of more tolerant water deficit stress genotypes alongside the identification of novel markers. However, the existent strategies contributing to this phenotype need to be identified and pooled according to standardized protocols and experiments.

Picoli et al. (2021) and Pita-Barbosa et al. (2023) showed a vast number of traits expected to be evaluated in the search for water deficit tolerance in eucalypt. Nevertheless, the metabolome analysis and some markers were foreseen or exemplified. A thoughtful approach of the compounds across diverging genotypes and control and stress treatment enabled additional insights on the plant strategies to cope

with water deficit. Therefore, the approach presented in this paper can be extended to other plant species and be used in future breeding programs.

Eucalypts grown under optimal conditions generally presented higher levels of FPCs. These compounds have been extensively studied as feeding deterrents against mammalians and invertebrates in eucalypts. They contain formyl moieties that seem to be the functional group responsible for the antifeedant effect in herbivores. Therefore, the higher levels of these defensive compounds in well-watered eucalypts indicates a regular mechanism for pest resistance (Wallis et al., 2010).

Findings for the tolerant stressed plants were consistent with previous reports. Sarker and Oba (2020) recently showed that derivatives of benzoic acid (e.g., gallic acid), cinnamic acid (e.g., caffeic acid) and flavonoids were more abundant in drought-tolerant leafy vegetable amaranths than in other genotypes. Another study with two rice varieties showed that the content of gallic acid, chlorogenic acid and syringic acid increased in the drought-tolerant variety under stress, while reducing in the sensitive one (Khan et al., 2017). Similar findings were observed by Quan et al. (2016), with vanillic acid and *p*-hydroxybenzoic acid as potential markers for tolerance in rice. The biosynthesis of potent antioxidants such as phenolics can be a chemical mechanism to tolerate the deficit of water that excessively produces ROS. Exogenous gallic acid promoted seedling growth in both tolerant and sensitive wheat cultivars under water deficit conditions (Bhardwaj et al., 2015). Likewise, exogenous caffeic acid induced salinity tolerance in wheat by improving plant water relations (Mehmood et al., 2021).

Our study covered a vast number of compounds from different classes compared to previous reports on eucalypts that targeted specific classes of compounds. Correia et al. (2014) reported only the accumulation of abscisic acid in the leaves of two tolerant clones of *E. globulus* submitted to drought. An experiment with seedlings of *E. globulus* and *E. viminalis* demonstrated no changes in foliar levels of terpenes and FPCs in response to water deficit. Only total phenolics level was reduced in stressed plants (McKiernan et al., 2014). Activation of phenylpropanoid biosynthetic pathway under stress conditions resulted in the accumulation of phenolics. These compounds can indeed improve plant tolerance and adaptability possibly by acting as universal stress protectors due to their high antioxidant efficiency (Šamec et al., 2021; Wang et al., 2019).

The capacity of UPLC-MS and ^{1}H-NMR datasets in potentially classifying seedlings of commercial *Eucalyptus* clones was evaluated. Results from both technologies were complementary and in concordance. Supervised and unsupervised integrated analysis generated a comprehensive overview of the eucalypt water stress responses. Water limitation reprogrammed the metabolic pathways of clones differently. Therefore, clones differing in drought tolerance could be discriminated according to the leaf metabolome changes as induced by water deficit conditions and to be examined for other stress conditions in the future.

3. Conclusions

This study provides the first comparative metabolomics approach to differentiate juvenile *Eucalyptus* clones subjected to drought stress, in order to define biomarkers of tolerance to this adverse environmental condition a growing threat worldwide. Intrinsic metabolic features in well-watered seedlings of tolerant and sensitive clones enabled their discrimination. However, the plant's metabolic response to drought stress appeared to be complex and variable depending on their genetic background. The results obtained in this work allowed us to classify clones of the same species/hybrids according to their drought tolerance of potential to be used in breeding programs that produce large number of individuals from the same parents. Classification models obtained from both NMR and UPLC-MS datasets were further validated with noticeable fitness and predictability using an extra subset of samples subjected to PEG stress.

In summary, the tolerant plants exposed to water deficit accumulated arginine, gallic acid derivatives, caffeic acid and tannins. In contrast, stressed drought-sensitive clones were characterised by a significant reduction of glucose, inositol and shikimic acid (Fig. 6). Under optimal growth conditions, all clones were rich in FPCs, indicating an important ecological role for this class of compounds and has yet to be examined in other model plants.

The results obtained herein can be used for earlier identification of tolerant clones and to enhance the understanding of the correlation among detected molecular markers (metabolites) and drought tolerance. It has yet to be determined whether these metabolites function as markers (indicator of water deficit stress) and/or additionally can mitigate drought. Understanding mechanisms of enhancing plant resilience and identifying indicators for early selection criteria is of the utmost importance to improve plant survival. One tool to achieve this is by engineering eucalypt to overproduce or inhibit the biosynthesis of certain chemicals using silencing techniques. This can provide better insight on their role in drought acclimation in this important wood crop.

4. Experimental

4.1 Chemicals

Methanol-d4 (99.80% D), acetone-d6 (99.80% D) and hexamethyldisiloxane (HMDS) were purchased from Deutero GmbH (Kastellaun, Germany). For NMR quantification and calibration of chemical shifts, HMDS was added to a final concentration of 0.94 mM. Acetonitrile, methanol, and acetic acid (LC–MS Chromasolv grade) were obtained from Fluka Analytical Sigma-Aldrich (Munich, Germany), milliQ water was used for UPLC-MS analysis. Chromoband C18 ec (1 ml 100 mg^{-1}) cartridge was purchased from Macherey and Nagel (Düren, Germany). All other chemicals and standards were from Sigma Aldrich (St. Louis, MO, USA).

4.2 Plant material

Thirteen commercial clones of *Eucalyptus* spp. from Suzano S/A (Brazil) were used in this study (**Table 4**). Extra information on the clone identification and performance may not be disclosed according to a

confidentiality contract with the forestry company. Information on climate zone x genotype distribution may also be requested and will be evaluated according to company policy. Requests to access clones' data should be directed to Edival Zauza (edivalzauza@suzano.com.br).

Acclimatised seedlings (110 days old) were grown in pots for 12 weeks under well-watered (WW) and water-deficit (WD) conditions. The experiment was performed during the summer in a glass greenhouse in Cajuri, MG, Brazil (natural photoperiod, mean temperature: 25°C and 70% relative humidity) as previously described by (Corrêa et al., 2017). Briefly, WD plants were watered with only 100 ml per day, while WW plants were watered by overhead sprinkler irrigation (3 times a day) plus direct soil irrigation (twice a day) – standard nursery irrigation (Fig. 7). An additional PEG-induced drought stress treatment was conducted in parallel with seedlings of the same clones. These plants were exposed to 100 ml PEG-6000 (300 g/L) every other day, in addition to standard nursery irrigation. Metabolomics data from this subset were used to assess the statistical model's potential in predicting the stress effect on sensitive and tolerant clones.

More experiment details, physiologic and phenotypic data have been previously reported by Corrêa et al. (2017). Twenty fully expanded leaves from each plant were harvested, air-dried, and milled in liquid nitrogen using pestle and mortar. After homogenisation using a bead beater, samples were freeze-dried and stored at -80°C until further use.

4.3 NMR spectroscopy analysis

For NMR, 150 mg of ground tissue samples were extracted in 1.5 ml methanol for 10 min in an ultrasound bath. After centrifugation (5 min at 13000 *g*), supernatant (1 ml) was taken and dried under a stream of nitrogen. Pellets were redissolved in 800 µl CD_3OD containing HMDS (0.94 mM) and transferred to 5 mm NMR tubes for analysis.

All ^{1}H-NMR spectra were recorded on an Agilent (Varian) VNMRS 400 NMR spectrometer operating at a proton NMR frequency of 399.92. The spectra were referenced to internal HMDS at 0.062 ppm for ^{1}H-NMR and to CD_3OD signals at 49.0 ppm for ^{13}C-NMR. ^{1}H-NMR spectra were recorded with the following parameters: digital resolution 0.37 Hz/point (32 K complex data points), pulse width = 2 ls (45°), relaxation delay = 0.35 s, acquisition time = 3.1 s, number of transients = 1024. Zero filling up to 128 K and an exponential window function with lb = 0.4 was used prior to Fourier transformation.

For further compound characterisation, selected samples were submitted to 2D NMR experiments. These were recorded on an Agilent (Varian) VNMRS 600 NMR spectrometer (proton and carbon NMR frequency of 599.83 and 149.95, respectively) using standard CHEMPACK 4.1 pulse sequences (gDQCOSY, gHSQCAD, gHMBCAD) implemented in Varian VNMRJ 2.2C spectrometer software.

4.4 Liquid chromatography–mass spectrometry (UPLC–MS)

For UPLC-MS, 30 mg of dry powder was extracted with 1 ml water:methanol (50:50, v/v) containing 5 µg/mL umbelliferone (internal standard used to check quality of injection) for 10 min in an ultrasound bath. After centrifugation (5 min at 13000 *g*), supernatant (750 µl) was placed on a (100 mg) C18

cartridge preconditioned with methanol and water. Samples were then eluted using 750 µl of methanol in glass vials for analysis.

LC–MS were recorded with an LCQ Deca XP MAX system (ThermoElectron, San Jose, USA) equipped with an ESI source in negative ionization mode. LC separation was carried out on an Acquity UHPLC system (Waters) using a reversed-phase HSS T3 column (100 × 1.0 mm, particle size 1.8 µm; Waters). The following binary gradient at a flow rate of 0.15 mL/min and an injection volume of 10 µl was applied: 0 to 1 min, isocratic 95% A (water/formic acid, 99.8/0.2 [v/v]), 5% B (acetonitrile/formic acid, 99.8/0.2 [v/v]); 1 to 16 min, linear from 5 to 95% B; 16 to 20 min, isocratic 95% B. Spectra were acquired in centroid mode with spray voltage set to 4.0 kV, capillary temperature 275°C, sheath and auxiliary/sweep gas (nitrogen) at 40 (arbitrary units) and 10 (arbitrary units), respectively.

Further LC–MS were recorded with an Dionex UltiMate 3000 UHPLC system coupled to an Orbitrap Elite mass spectrometer (Thermo Fisher Scientific, Germany). LC separation was carried out on an RP-18 column (particle size 1.9 µm, pore size 175 Å, 50 × 2.1 mm ID, Hypersil GOLD, Thermo Fisher Scientific; column temperature 40°C) using the same binary gradient and flow rate described for the LCQ Deca XP MAX system, but with an injection volume of 2 µl. Mass spectra were collected in negative ion mode with a heated ESI source at 250°C, spray voltage 4.0 kV, capillary temperature 275°C, FTMS resolution 15,000, sheath and auxiliary gas (nitrogen) at 30 (arbitrary units) and 15 (arbitrary units), respectively. The CID mass spectra (buffer gas: helium) were recorded using normalized collision energy of 35%. The data were evaluated using the software Xcalibur 2.2 SP1.48.

Metabolite assignments were made by comparing Rt, UV/Vis spectra and MS data (accurate mass, isotopic distribution, and fragmentation pattern) of the detected metabolites with the reported data in the literature for *Eucalyptus* samples, and in some databases (e.g. the dictionary of natural products database (Wiley, CRC), Reaxys and Scifinder). Identifications were confirmed with authentic standards whenever available in-house.

4.5 UPLC-MS and NMR data processing and multivariate data analysis

Native LC–MS files were converted into .netCDF and .mzML files. Relative quantification and comparison of *Eucalyptus* metabolites after LC–MS was performed using XCMS data analysis software, under R Studio environment (Smith et al., 2006) using custom-written procedures. This software approach employs peak alignment, matching and comparison as described elsewhere (Farag et al., 2015).

The ^{1}H-NMR spectra were automatically Fourier transformed to ESP files using ACD/NMR Manager lab version 10.0 software (Toronto, Canada). Spectral intensities were reduced to integrated regions, referred to as buckets, of equal width (0.04 ppm) within the region of δ_H 11.4 to -0.4 ppm. The regions between δ_H 5.0-4.7 and 3.4-3.25 ppm corresponding to residual water and methanol signals, respectively, were removed prior to multivariate analyses.

The resulting peak list was processed using Microsoft Excel software (Microsoft, Redmond, WA), where the ion features were normalised to the total integrated area (1000) per sample (UPLC-MS data)

and the chemical shifts were scaled to HMDS signal (^{1}H-NMR data). These lists were analysed using SIMCA-P 14.1 software package (Umetrics, Umea, Sweden), where the data was subjected to principal component analysis (PCA) and orthogonal projections to latent structures-discriminant analysis (OPLS-DA). All variables were mean centred and scaled to Pareto variance.

Author contributions

C. Noleto-Dias performed the sample preparation and data analysis and drafted the manuscript. E. Picoli performed the drought experiment. C. Noleto-Dias, A. Porzel, L. Wessjohann and M. Farag contributed to the data interpretation and discussion of the results. E. Picoli and J. Tavares contributed to the original idea and research design; All authors reviewed the manuscript.

Acknowledgments

We are grateful to Suzano S/A for providing the seedlings of *Eucalyptus* hybrids. Dr Mohamed A. Farag acknowledges the funding received by the Alexander von Humboldt foundation, Germany. This study was supported by grants from CAPES, CNPq, and FAPEMIG through the award of a scholarship and financial support. We are grateful to Ms. Anja Ehrlich and Ms. Annegret Laub for assistance in running the UPLC-MS batches.

Supplementary material

Additional supporting information may be found online in the Supporting Information section.

References

Abid, G., Silue, S., Muhovski, Y., Jacquemin, J.-M., Toussaint, A., Baudoin, J.-P., 2009. Role of myo-inositol phosphate synthase and sucrose synthase genes in plant seed development. Gene 439, 1–10. https://doi.org/10.1016/j.gene.2009.03.007

Amakura, Y., Yoshimura, M., Sugimoto, N., Yamazaki, T., Yoshida, T., 2009. Marker constituents of the natural antioxidant *Eucalyptus* leaf extract for the evaluation of food additives. Biosci. Biotechnol. Biochem. 73, 1060–1065. https://doi.org/10.1271/bbb.80832

Amaral, D.C., Brown, P.H., 2022. Foliar application of an inositol-based plant biostimulant boosts zinc accumulation in wheat grains: A μ-X-Ray fluorescence case study. Front. Plant Sci. 13. https://doi.org/10.3389/fpls.2022.837695

Arndt, S.K., Livesley, S.J., Merchant, A., Bleby, T.M., Grierson, P.., 2008. Quercitol and

osmotic adaptation of field-grown *Eucalyptus* under seasonal drought stress. Plant. Cell Environ. 31, 915–924. https://doi.org/10.1111/j.1365-3040.2008.01803.x

Battie-Laclau, P., Laclau, J., Domec, J., Christina, M., Bouillet, J., Cassia Piccolo, M., Moraes Gonçalves, J.L., Moreira, R.M. e, Krusche, A.V., Bouvet, J., Nouvellon, Y., 2014. Effects of potassium and sodium supply on drought-adaptive mechanisms in *Eucalyptus grandis* plantations. New Phytol. 203, 401–413. https://doi.org/10.1111/nph.12810

Bhardwaj, R.D., Sharma, A., Sharma, H., Srivastava, P., 2015. Role of gallic acid pre-treatment in inducing the antioxidant response of two wheat cultivars differing in drought tolerance. Indian J. Agric. Biochem. 28, 155. https://doi.org/10.5958/0974-4479.2015.00010.6

Bijttebier, S., Van der Auwera, A., Foubert, K., Voorspoels, S., Pieters, L., Apers, S., 2016. Bridging the gap between comprehensive extraction protocols in plant metabolomics studies and method validation. Anal. Chim. Acta 935, 136–150. https://doi.org/10.1016/j.aca.2016.06.047

Bolte, M.L., Bowers, J., Crow, W.D., Paton, D.M., Sakurai, A., Takahashi, N., Ujiie, M., Yoshida, S., 1984. Germination inhibitor from *Eucalyptus pulverulenta*. Agric. Biol. Chem. 48, 373–376. https://doi.org/10.1080/00021369.1984.10866137

Booth, T.H., 2013. Eucalypt plantations and climate change. For. Ecol. Manage. 301, 28–34. https://doi.org/10.1016/j.foreco.2012.04.004

Brereton, R.G., 2003. Chemometrics: data analysis for the laboratory and chemical plant. Wiley, Chichester, England.

Çevik, S., Yıldızlı, A., Yandım, G., Göksu, H., Gultekin, M.S., Güzel Değer, A., Çelik, A., Şimşek Kuş, N., Ünyayar, S., 2014. Some synthetic cyclitol derivatives alleviate the effect of water deficit in cultivated and wild-type chickpea species. J. Plant Physiol. 171, 807–816. https://doi.org/10.1016/j.jplph.2014.01.010

Chatara, T., Musvosvi, C., Houdegbe, A.C., Sibiya, J., 2023. Variance components, correlation and path coefficient analysis of morpho-physiological and yield related traits in spider

plant (*Gynandropsis gynandra* (L.) Briq.) under water-stress conditions. Agronomy 13, 752. https://doi.org/10.3390/agronomy13030752

Chenavas, S., Fiorini-Puybaret, C., Joulia, P., Larrouquet, C., Waton, H., Martinez, A., Casabianca, H., Fabre, B., 2015. New formylated phloroglucinol compounds from *Eucalyptus globulus* foliage. Phytochem. Lett. 11, 69–73. https://doi.org/10.1016/j.phytol.2014.11.002

Cheng, Q., Snyder, J.K., 1991. Two new phloroglucinol derivatives with phosphodiesterase inhibitory activity from the leaves of *Eucalyptus robusta*. Zeitschrift für Naturforsch. B 46, 1275–1277.

Condé, S.A., Picoli, E.A.T., Corrêa, T.R., Dias, L.A.S., Lourenço, R.D.S., Silva, F.C.S., Pereira, W.L., Zauza, E.A.V., 2020. Biomarkers for early selection in *Eucalyptus* tolerant to dieback associated with water deficit. Rev. Bras. Ciências Agrárias - Brazilian J. Agric. Sci. 15, 1–10. https://doi.org/10.5039/agraria.v15i3a7515

Cook, R.L., Binkley, D., Stape, J.L., 2016. *Eucalyptus* plantation effects on soil carbon after 20 years and three rotations in Brazil. For. Ecol. Manage. 359, 92–98. https://doi.org/10.1016/j.foreco.2015.09.035

Corrêa, T.R., Picoli, E.A. de T., Pereira, W.L., Condé, S.A., Resende, R.T., de Resende, M.D. V., da Costa, W.G., Cruz, C.D., Zauza, E.A. V., 2023. Very early biomarkers screening for water deficit tolerance in commercial *Eucalyptus* clones. Agronomy 13, 937. https://doi.org/10.3390/agronomy13030937

Corrêa, T.R., Picoli, E.A. de T., Souza, G.A. de, Condé, S.A., Silva, N.M., Lopes-Mattos, K.L.B., Resende, M.D.V. de, Zauza, E.A.V., Oda, S., 2017. Phenotypic markers in early selection for tolerance to dieback in *Eucalyptus*. Ind. Crops Prod. 107, 130–138. https://doi.org/10.1016/j.indcrop.2017.05.032

Correia, B., Hancock, R.D., Amaral, J., Gomez-Cadenas, A., Valledor, L., Pinto, G., 2018. Combined drought and heat activates protective responses in *Eucalyptus globulus* that are

not activated when subjected to drought or heat stress alone. Front. Plant Sci. 9. https://doi.org/10.3389/fpls.2018.00819

Correia, B., Pintó-Marijuan, M., Neves, L., Brossa, R., Dias, M.C., Costa, A., Castro, B.B., Araújo, C., Santos, C., Chaves, M.M., Pinto, G., 2014. Water stress and recovery in the performance of two *Eucalyptus globulus* clones: physiological and biochemical profiles. Physiol. Plant. 150, 580–592. https://doi.org/10.1111/ppl.12110

Dias, C.N., Picoli, E.A. de T., Souza, G.A. de, Farag, M.A., Scotti, M.T., Filho, J.M.B., Silva, M.S. da, Tavares, J.F., 2017. Phenolics metabolism provides a tool for screening drought tolerant *Eucalyptus grandis* hybrids. Aust. J. Crop Sci. 11, 1016–1024.

Duursma, R.A., Barton, C.V.M., Eamus, D., Medlyn, B.E., Ellsworth, D.S., Forster, M.A., Tissue, D.T., Linder, S., McMurtrie, R.E., 2011. Rooting depth explains [CO2] x drought interaction in *Eucalyptus saligna*. Tree Physiol. 31, 922–931. https://doi.org/10.1093/treephys/tpr030

Farag, M.A., Deavours, B.E., de Fátima, A., Naoumkina, M., Dixon, R.A., Sumner, L.W., 2009. Integrated metabolite and transcript profiling identify a biosynthetic mechanism for hispidol in *Medicago truncatula* cell cultures. Plant Physiol. 151, 1096–1113. https://doi.org/10.1104/pp.109.141481

Farag, M.A., Kabbash, E.M., Mediani, A., Döll, S., Esatbeyoglu, T., Afifi, S.M., 2022. Comparative metabolite fingerprinting of four different *Cinnamon* species analyzed via UPLC–MS and GC–MS and chemometric tools. Molecules 27, 2935. https://doi.org/10.3390/molecules27092935

Farag, M.A., Porzel, A., Mahrous, E.A., El-Massry, M.M., Wessjohann, L.A., 2015. Integrated comparative metabolite profiling via MS and NMR techniques for Senna drug quality control analysis. Anal. Bioanal. Chem. 407, 1937–1949. https://doi.org/10.1007/s00216-014-8432-1

Florêncio, G.W.L., Martins, F.B., Fagundes, F.F.A., 2022. Climate change on *Eucalyptus*

plantations and adaptive measures for sustainable forestry development across Brazil. Ind. Crops Prod. 188, 115538. https://doi.org/10.1016/j.indcrop.2022.115538

Gill, S.S., Tuteja, N., 2010. Reactive oxygen species and antioxidant machinery in abiotic stress tolerance in crop plants. Plant Physiol. Biochem. https://doi.org/10.1016/j.plaphy.2010.08.016

Gromski, P.S., Muhamadali, H., Ellis, D.I., Xu, Y., Correa, E., Turner, M.L., Goodacre, R., 2015. A tutorial review: Metabolomics and partial least squares-discriminant analysis – a marriage of convenience or a shotgun wedding. Anal. Chim. Acta 879, 10–23. https://doi.org/10.1016/j.aca.2015.02.012

Hasegawa, T., Takano, F., Takata, T., Niiyama, M., Ohta, T., 2008. Bioactive monoterpene glycosides conjugated with gallic acid from the leaves of *Eucalyptus globulus*. Phytochemistry 69, 747–753. https://doi.org/10.1016/j.phytochem.2007.08.030

Hongcheng, W., Fujimotot, Y., 1993. Triterpene esters from *Eucalyptus tereticornis*. Phytochemistry 33, 151–153. https://doi.org/10.1016/0031-9422(93)85412-K

Hussein, H.-A.A., Alshammari, S.O., Kenawy, S.K.M., Elkady, F.M., Badawy, A.A., 2022. Grain-priming with L-arginine improves the growth performance of wheat (*Triticum aestivum* L.) plants under drought stress. Plants 11, 1219. https://doi.org/10.3390/plants11091219

IBGE, 2021. Florestas plantadas no Brasil somam 9,3 milhões de hectares em 2020 [WWW Document]. URL https://agenciabrasil.ebc.com.br/geral/noticia/2021-10/florestas-plantadas-no-brasil-somam-93-milhoes-de-hectares-em-2020 (accessed 9.20.22).

Jia, Q., Kong, D., Li, Q., Sun, S., Song, J., Zhu, Y., Liang, K., Ke, Q., Lin, W., Huang, J., 2019. The function of inositol phosphatases in plant tolerance to abiotic stress. Int. J. Mol. Sci. 20, 3999. https://doi.org/10.3390/ijms20163999

Khan, F., Upreti, P., Singh, R., Shukla, P.K., Shirke, P.A., 2017. Physiological performance of two contrasting rice varieties under water stress. Physiol. Mol. Biol. Plants 23, 85–97.

https://doi.org/10.1007/s12298-016-0399-2

Lemcoff, J.H., Guarnaschelli, A.B., Garau, A.M., Bascialli, M.E., Ghersa, C.M., 1994. Osmotic adjustment and its use as a selection criterion in *Eucalyptus* seedlings. Can. J. For. Res. 24, 2404–2408. https://doi.org/10.1139/x94-310

Mahajan, S., Mahajan, S., Tuteja, N., Tuteja, N., 2005. Cold, salinity and drought stresses: an overview. Arch. Biochem. Biophys. 444, 139–58. https://doi.org/10.1016/j.abb.2005.10.018

Marsh, K.J., Kulheim, C., Blomberg, S.P., Thornhill, A.H., Miller, J.T., Wallis, I.R., Nicolle, D., Salminen, J.-P., Foley, W.J., 2017. Genus-wide variation in foliar polyphenolics in eucalypts. Phytochemistry 144, 197–207. https://doi.org/10.1016/j.phytochem.2017.09.014

McKiernan, A.B., Hovenden, M.J., Brodribb, T.J., Potts, B.M., Davies, N.W., O'Reilly-Wapstra, J.M., 2014. Effect of limited water availability on foliar plant secondary metabolites of two *Eucalyptus* species. Environ. Exp. Bot. 105, 55–64. https://doi.org/10.1016/j.envexpbot.2014.04.008

Mehmood, H., Abbasi, G.H., Jamil, M., Malik, Z., Ali, M., Iqbal, R., 2021. Assessing the potential of exogenous caffeic acid application in boosting wheat (*Triticum aestivum* L.) crop productivity under salt stress. PLoS One 16, e0259222. https://doi.org/10.1371/journal.pone.0259222

Merchant, A., Callister, A., Arndt, S., Tausz, M., Adams, M., 2007. Contrasting physiological responses of six *Eucalyptus* species to water deficit. Ann. Bot. 100, 1507–1515. https://doi.org/10.1093/aob/mcm234

Merchant, A., Richter, A.A., 2011. Polyols as biomarkers and bioindicators for 21st century plant breeding. Funct. Plant Biol. 38, 934–940. https://doi.org/10.1071/FP11105

Mircea, D.M., Calone, R., Shakya, R., Saavedra, M.F., Sestras, R.E., Boscaiu, M., Sestras, A.F., Vicente, O., 2023. Use of multivariate analysis in screening for drought tolerance in

ornamental Asteraceae species. Agronomy 13, 687. https://doi.org/10.3390/agronomy13030687

Nolan, R.H., Gauthey, A., Losso, A., Medlyn, B.E., Smith, R., Chhajed, S.S., Fuller, K., Song, M., Li, X., Beaumont, L.J., Boer, M.M., Wright, I.J., Choat, B., 2021. Hydraulic failure and tree size linked with canopy die-back in eucalypt forest during extreme drought. New Phytol. 230, 1354–1365. https://doi.org/10.1111/nph.17298

Noleto-Dias, C., Ward, J.L., Bellisai, A., Lomax, C., Beale, M.H., 2018. Salicin-7-sulfate: A new salicinoid from willow and implications for herbal medicine. Fitoterapia 127, 166–172. https://doi.org/10.1016/j.fitote.2018.02.009

Oberschelp, G.P.J., Morales, L.L., Montecchiarini, M.L., Harrand, L., Podestá, F.E., Margarit, E., 2022. Harder, better, faster, stronger: Frost tolerance of *Eucalyptus benthamii* under cold acclimation. Plant Physiol. Biochem. 186, 64–75. https://doi.org/10.1016/j.plaphy.2022.06.022

Picoli, E.A.T., Resende, M.D. V, Oda, S., 2021. Come hell or high water: breeding the profile of *Eucalyptus* tolerance to abiotic stress focusing water deficit. pp. 91–127. https://doi.org/10.1007/978-3-030-78420-1_5

Pita-Barbosa, A., Oliveira, L.A., de Barros, N.F., Hodecker, B.E.R., Oliveira, F.S., Araújo, W.L., Martins, S.C. V, 2023. Developing a roadmap to define a potential ideotype for drought tolerance in *Eucalyptus*. For. Sci. 69, 101–114. https://doi.org/10.1093/forsci/fxac044

Quan, N., Anh, L., Khang, D., Tuyen, P., Toan, N., Minh, T., Minh, L., Bach, D., Ha, P., Elzaawely, A., Khanh, T., Trung, K., Xuan, T., 2016. Involvement of secondary metabolites in response to drought stress of rice (*Oryza sativa* L.). Agriculture 6, 23. https://doi.org/10.3390/agriculture6020023

Sala, A., Piper, F., Hoch, G., 2010. Physiological mechanisms of drought-induced tree mortality are far from being resolved. New Phytol. 186, 274–281. https://doi.org/10.1111/j.1469-

8137.2009.03167.x

Šamec, D., Karalija, E., Šola, I., Vujčić Bok, V., Salopek-Sondi, B., 2021. The role of polyphenols in abiotic stress response: The influence of molecular structure. Plants 10, 118. https://doi.org/10.3390/plants10010118

Santos, S.A.O.O., Vilela, C., Freire, C.S.R.R., Neto, C.P., Silvestre, A.J.D.D., 2013. Ultra-high performance liquid chromatography coupled to mass spectrometry applied to the identification of valuable phenolic compounds from *Eucalyptus* wood. J. Chromatogr. B 938, 65–74. https://doi.org/10.1016/j.jchromb.2013.08.034

Sarker, U., Oba, S., 2020. Phenolic profiles and antioxidant activities in selected drought-tolerant leafy vegetable amaranth. Sci. Rep. 10, 18287. https://doi.org/10.1038/s41598-020-71727-y

Serag, A., Zayed, A., Mediani, A., Farag, M.A., 2023. Integrated comparative metabolite profiling via NMR and GC–MS analyses for tongkat ali (*Eurycoma longifolia*) fingerprinting and quality control analysis. Sci. Rep. 13, 2533. https://doi.org/10.1038/s41598-023-28551-x

Shvaleva, A.L., Silva, F.C.E., Breia, E., Jouve, J., Hausman, J.F., Almeida, M.H., Maroco, J.P., Rodrigues, M.L., Pereira, J.S., Chaves, M.M., 2006. Metabolic responses to water deficit in two *Eucalyptus globulus* clones with contrasting drought sensitivity. Tree Physiol. 26, 239–248. https://doi.org/10.1093/treephys/26.2.239

Sidana, J., Foley, W.J., Singh, I.P., 2012. Isolation and quantitation of ecologically important phloroglucinols and other compounds from *Eucalyptus jensenii*. Phytochem. Anal. 23, 483–491. https://doi.org/10.1002/pca.2345

Silveira, N.M., Ribeiro, R. V., de Morais, S.F.N., de Souza, S.C.R., da Silva, S.F., Seabra, A.B., Hancock, J.T., Machado, E.C., 2021. Leaf arginine spraying improves leaf gas exchange under water deficit and root antioxidant responses during the recovery period. Plant Physiol. Biochem. 162, 315–326. https://doi.org/10.1016/j.plaphy.2021.02.036

Smith, C.A., Want, E.J., O'Maille, G., Abagyan, R., Siuzdak, G., 2006. XCMS: Processing mass spectrometry data for metabolite profiling using nonlinear peak alignment, matching, and identification. Anal. Chem. 78, 779–787. https://doi.org/10.1021/ac051437y

Talhaoui, N., Gómez-Caravaca, A.M., Roldán, C., León, L., De la Rosa, R., Fernández-Gutiérrez, A., Segura-Carretero, A., 2015. Chemometric analysis for the evaluation of phenolic patterns in olive leaves from six cultivars at different growth stages. J. Agric. Food Chem. 63, 1722–1729. https://doi.org/10.1021/jf5058205

Tomé, M., Almeida, M.H., Barreiro, S., Branco, M.R., Deus, E., Pinto, G., Silva, J.S., Soares, P., Rodríguez-Soalleiro, R., 2021. Opportunities and challenges of *Eucalyptus* plantations in Europe: the Iberian Peninsula experience. Eur. J. For. Res. 140, 489–510. https://doi.org/10.1007/s10342-021-01358-z

Tuominen, A., Toivonen, E., Mutikainen, P., Salminen, J.-P., 2013. Defensive strategies in *Geranium sylvaticum*. Part 1: Organ-specific distribution of water-soluble tannins, flavonoids and phenolic acids. Phytochemistry 95, 394–407. https://doi.org/10.1016/j.phytochem.2013.05.013

Valladares, F., Gianoli, E., Gómez, J.M., 2007. Ecological limits to plant phenotypic plasticity. New Phytol. 176, 749–763. https://doi.org/10.1111/j.1469-8137.2007.02275.x

Villate, A., San Nicolas, M., Gallastegi, M., Aulas, P.-A., Olivares, M., Usobiaga, A., Etxebarria, N., Aizpurua-Olaizola, O., 2021. Review: Metabolomics as a prediction tool for plants performance under environmental stress. Plant Sci. 303, 110789. https://doi.org/10.1016/j.plantsci.2020.110789

Wallis, I.R., Smith, H.J., Henery, M.L., Henson, M., Foley, W.J., 2010. Foliar chemistry of juvenile *Eucalyptus grandis* clones does not predict chemical defence in maturing ramets. For. Ecol. Manage. 260, 763–769. https://doi.org/10.1016/j.foreco.2010.05.034

Wang, J., Yuan, B., Huang, B., 2019. Differential heat-induced changes in phenolic acids associated with genotypic variations in heat tolerance for hard fescue. Crop Sci. 59, 667–

674. https://doi.org/10.2135/cropsci2018.01.0063

You, J., Zhang, Yujuan, Liu, A., Li, D., Wang, X., Dossa, K., Zhou, R., Yu, J., Zhang, Yanxin, Wang, L., Zhang, X., 2019. Transcriptomic and metabolomic profiling of drought-tolerant and susceptible sesame genotypes in response to drought stress. BMC Plant Biol. 19, 267. https://doi.org/10.1186/s12870-019-1880-1

Zhang, Y., Wang, X., 2021. Geographical spatial distribution and productivity dynamic change of eucalyptus plantations in China. Sci. Rep. 11, 19764. https://doi.org/10.1038/s41598-021-97089-7

Figures

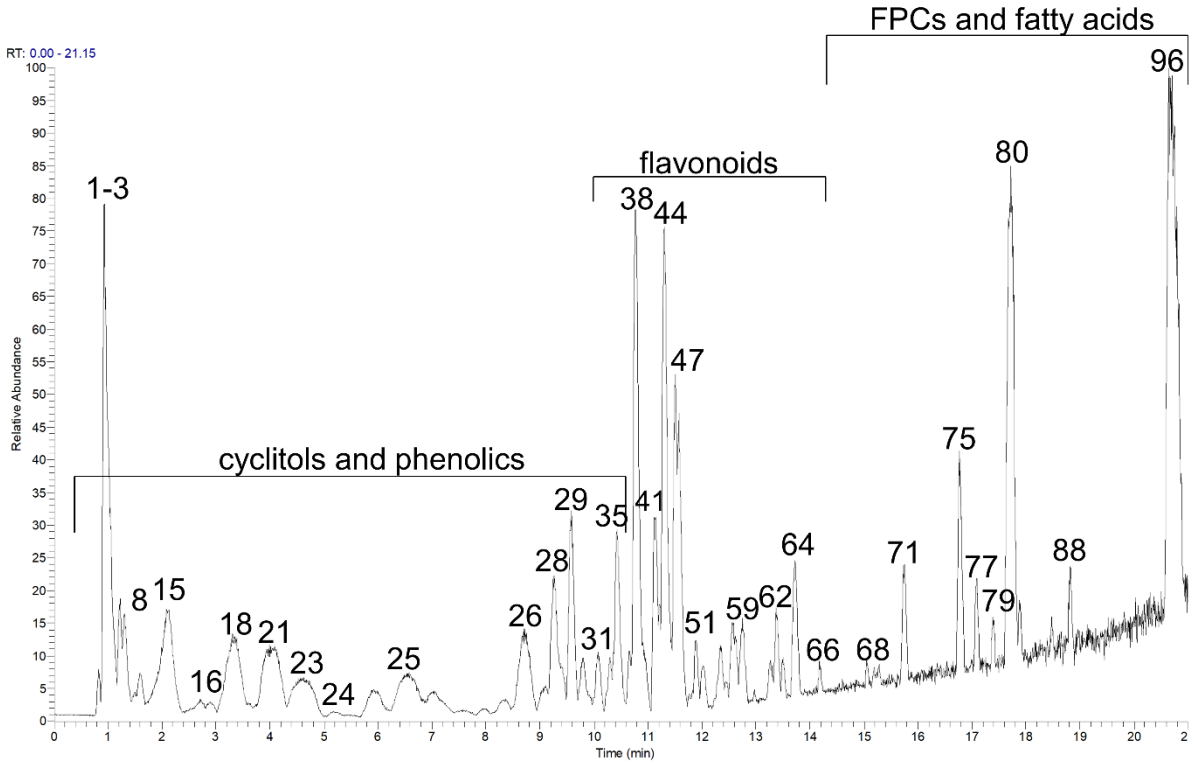

Fig. 1. UPLC-MS base peak chromatograms of the *Eucalyptus* spp. leaf extract in negative ion mode. Numbers correspond to the peak no. in Table 1. Chromatographic conditions were as indicated in the Experimental section. The identities, retention time, and basic UV and MS data of all peaks are listed in Table 1. FPCs – formylated phloroglucinol compounds.

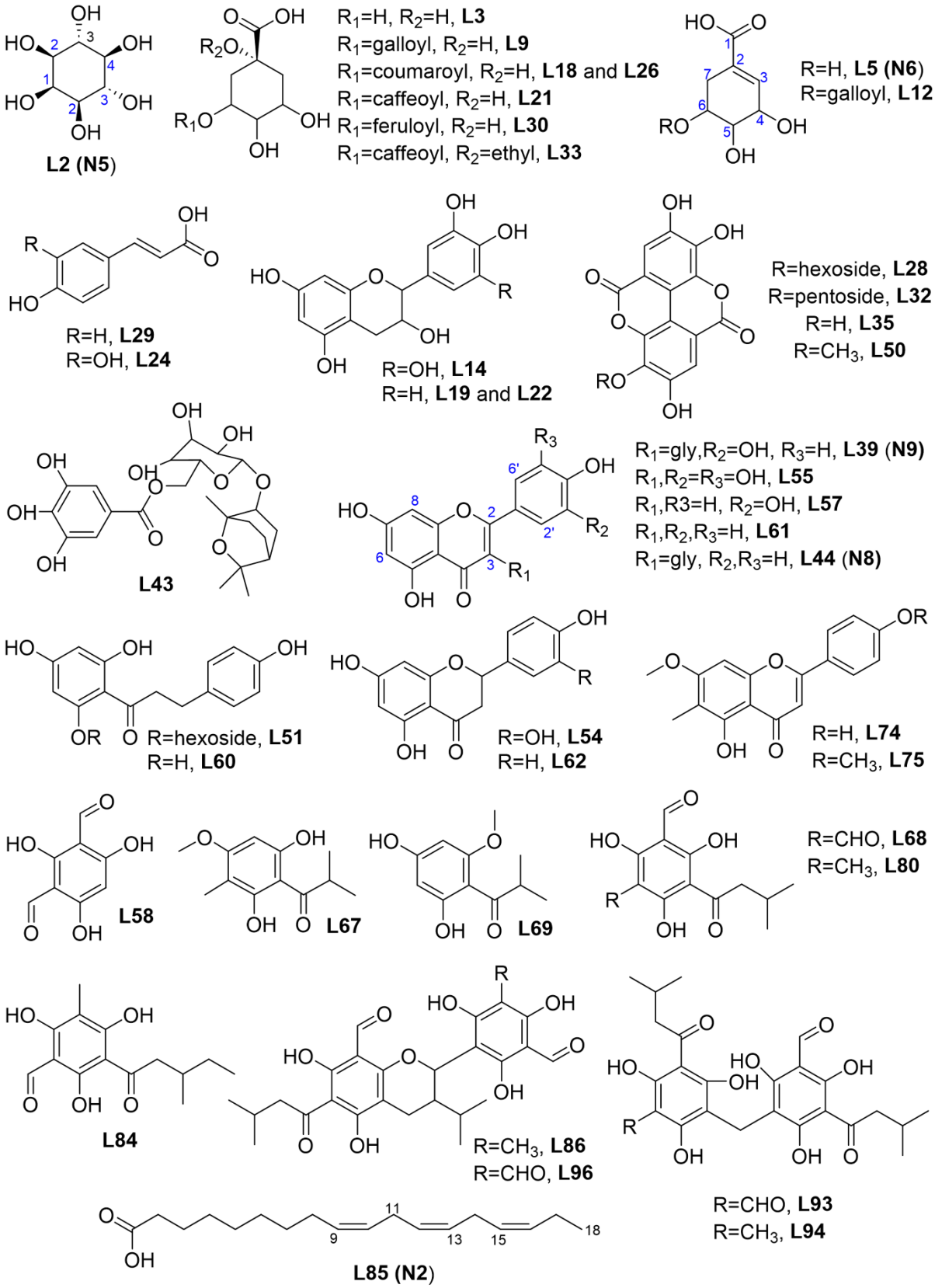

Fig 2. Molecular features identified in the methanol extract of *Eucalyptus* spp. leaves. Numbering refers to Table 1 and 2. Note the carbon numbering system in blue for the compounds is used throughout the manuscript for NMR assignments and thus is based on analogy rather than IUPAC rules.

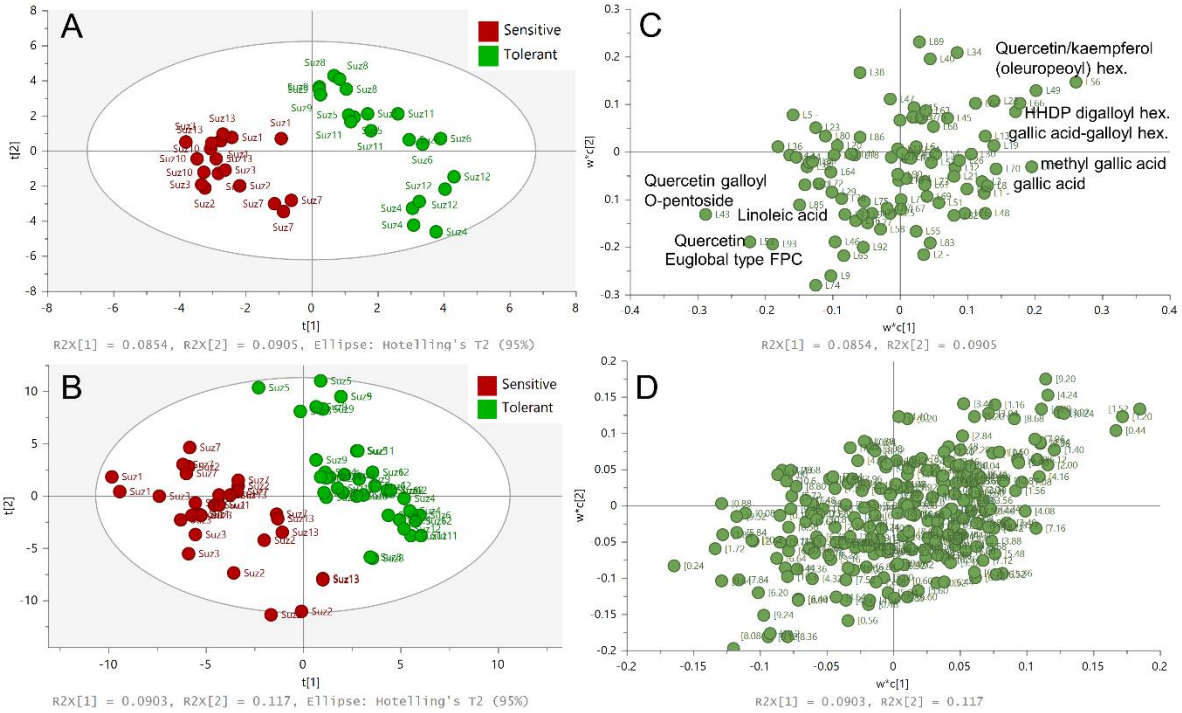

Fig. 3. Partial least squares-discriminant analysis (PLS-DA) scores and loadings plot of the UPLC-MS (A/C) and ^{1}H-NMR (B/D) datasets derived from leaf extracts of seedlings of 13 commercial eucalypt clones grown at well-watered condition. Clones are coloured according to their response to drought (sensitive and tolerant).

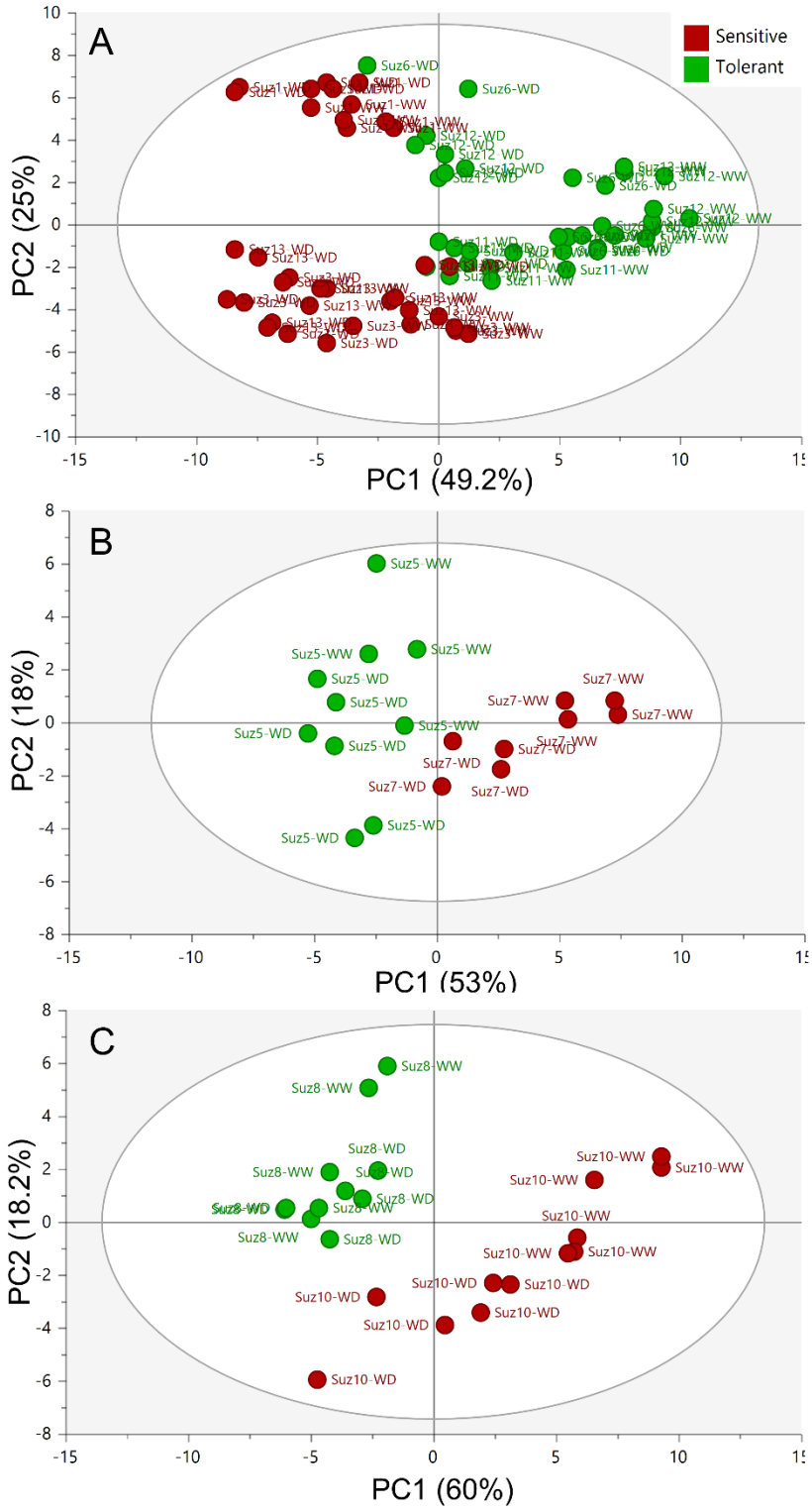

Fig. 4. Principal Component Analysis (PCA) scores plots indicating separation of *Eucalyptus* clones sensitive and tolerant to drought mostly in the direction of PC1 (ca. 50%). (A) *E. grandis* × *urophylla;* (B) *E. grandis* × *pellita*; and (C) *E. grandis.* Clones are coloured according to their response to drought (sensitive and tolerant).

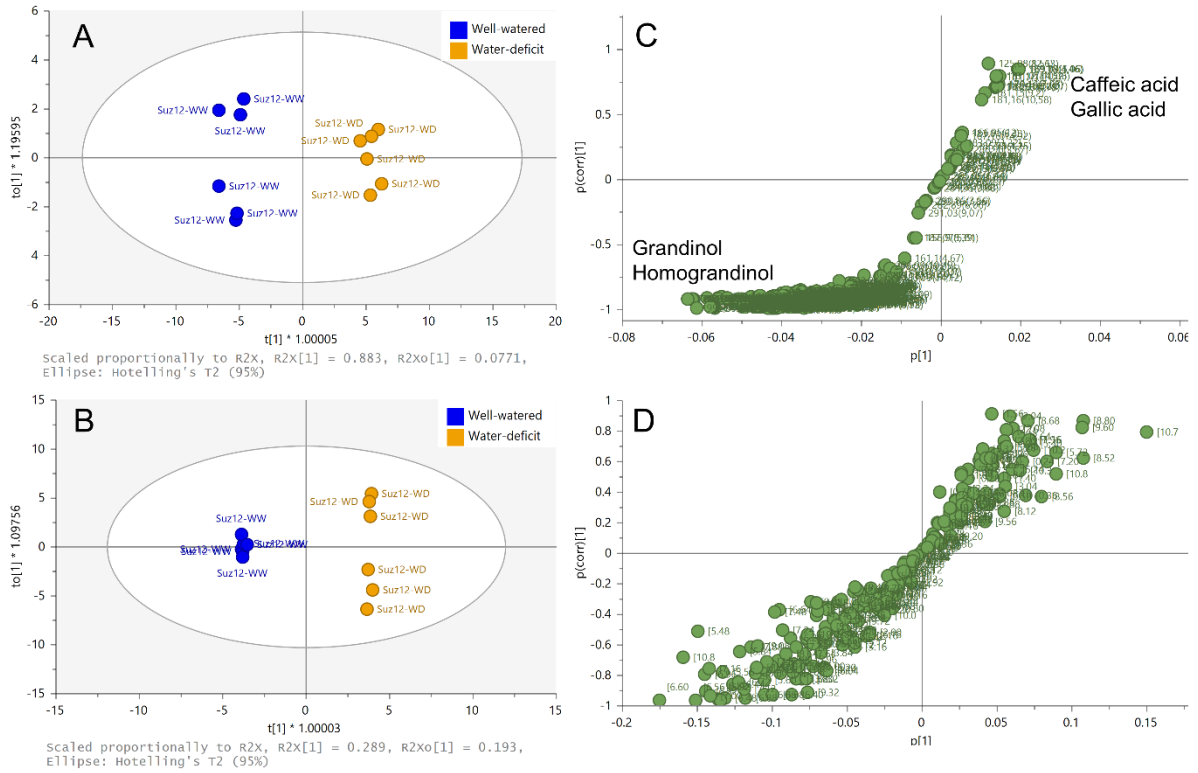

Fig. 5. Orthogonal partial least squares discriminant analysis (OPLS-DA) scores and S-plots of the UPLC-MS (A/C) and ^{1}H-NMR (B/D) datasets of the drought tolerant clone Suz12 (*Eucalyptus. grandis* × *urophylla*). Samples are coloured according to their growth conditions.

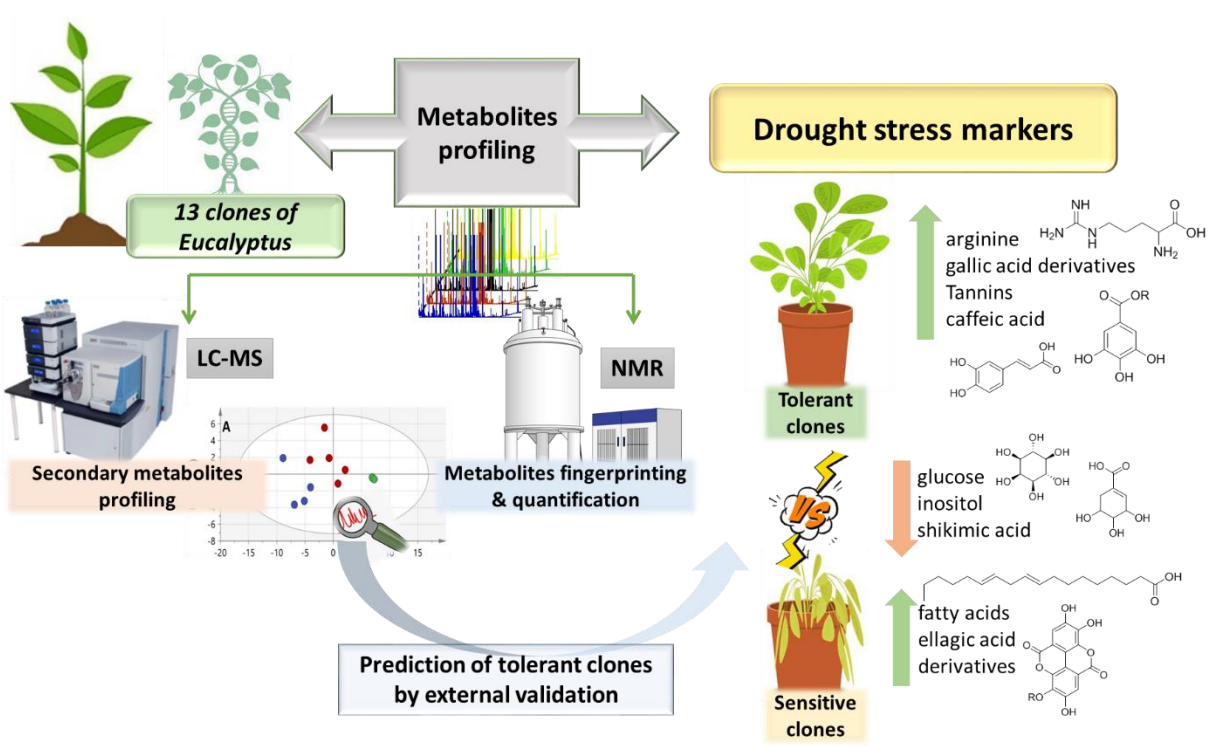

Fig. 6. Study design and main markers identified in tolerant versus sensitive clones using NMR and UPLC-MS metabolomics approaches. Up and down arrows indicate for chemicals showing increase versus decrease in respective clones.

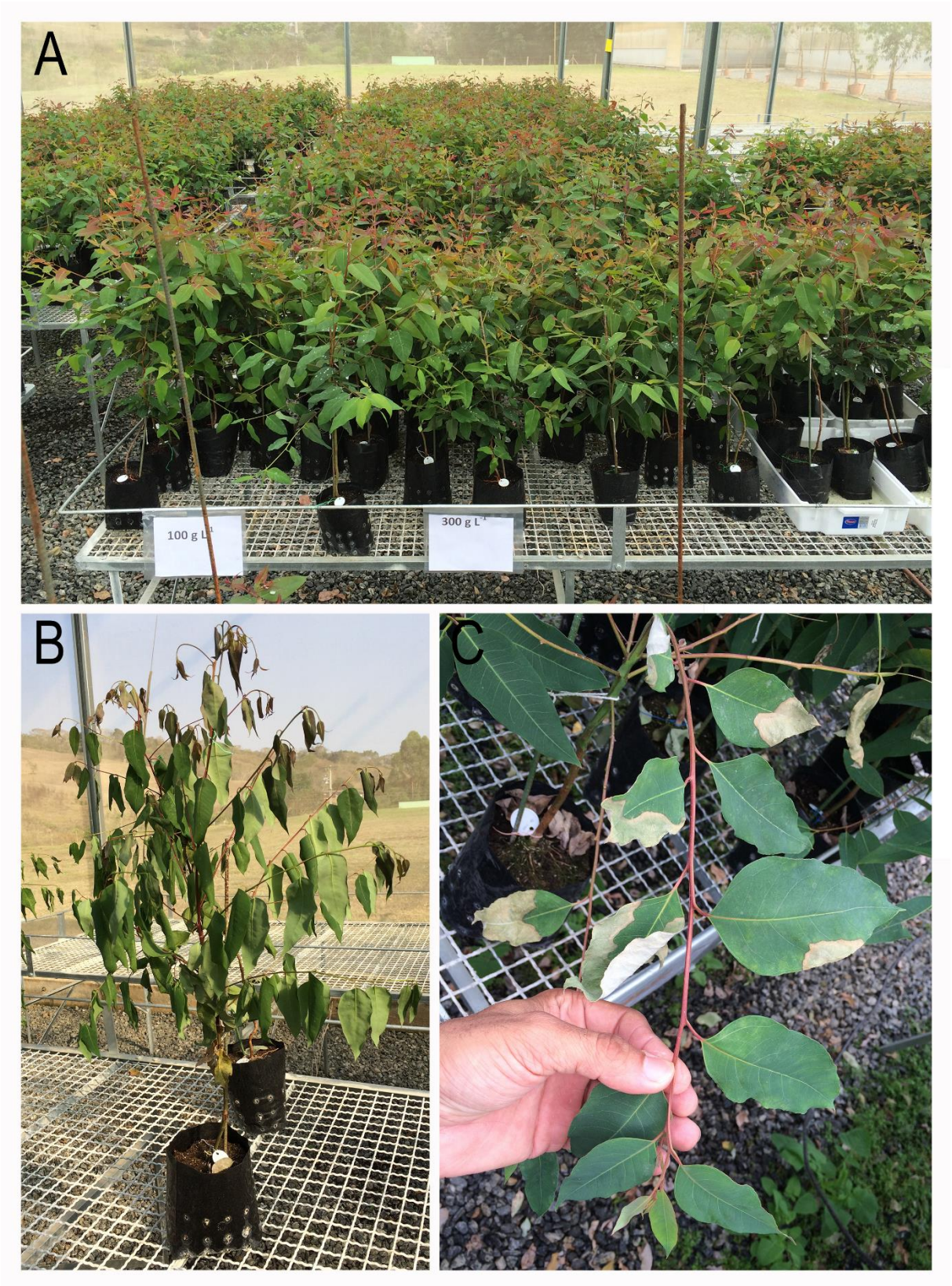

Fig. 7. Partial view and plant details/water deficit symptoms in the experiment simulating water deficit. (A) Partial view of the experiment plots inside the greenhouse; (B) water deficit symptoms, plant wilting due to the water deficit treatment, and (C) water deficit symptoms, leaf necrosis at the leaf apex and borders.

Tables

Table 1. Peak assignments in Eucalyptus spp. leaf extract via UPLC-MS in negative ionization mode.

Peak no.	**[M-H]$^-$** (*m/z*)	**Rt** (min)	**UV** (nm)	**Molecular formula**	**Error** (ppm)	**MS/MS product ions** (*m/z*)	**Identification**	**Classes**
L1	173.1048	0.86	225, 263	$C_6H_{14}N_4O_2$	+2.5	-	Arginine	Amino acid
L2	179.0565	0.90	225, 263	$C_6H_{12}O_6$	+2.3	87, 117, 125, 143, 151, **161**	*myo*-inositol*	Cyclitol
L3	191.0562	0.94	225, 263	$C_7H_{12}O_6$	+0.3	85, **111**, 127, 143, 155, 173	Quinic acid	Cyclitol
L4	331.0673	1.02	263, 369	$C_{13}H_{16}O_{10}$	+0.6	125, **169**	Glucogallin	Gallotannin
L5	173.0457	1.03	263, 369	$C_7H_{10}O_5$	+1.0	111, 137, **155**	Shikimic acid	Cyclitol
L6	481.0621	1.22	263, 369	$C_{20}H_{18}O_{14}$	-0.6	205, 275, **300.9**	HHDP *O*-hexoside	Ellagitannin
L7	633.0729	1.24	366	$C_{27}H_{22}O_{18}$	-0.7	203, 231, 249, 275, **300.9**, 421, 481, 614	HHDP galloyl *O*-hexoside	Ellagitannin
L8	130.0877	1.25	366	$C_6H_{13}NO_2$	+3.0	-	Leucine	Amino acid
L9	343.0673	1.27	366, 377	$C_{14}H_{16}O_{10}$	+0.6	125, 169, 173, **191**, 282, 295, 325	Galloylquinic acid	Cyclitol phenolic acid
L10	169.0144	1.28	298, 384	$C_7H_6O_5$	+1.0	81, 97, **125**, 151	Gallic acid*	Phenolic acid
L11	483.0778	1.38	272, 351	$C_{20}H_{20}O_{14}$	-0.5	**169**, 271, 313, 331	Digalloyl *O*-hexoside isomer	Gallotannin
L12	325.0565	1.47	267, 369	$C_{14}H_{14}O_9$	+0.1	125, 155, **169**, 173, 237, 263, 281, 289, 307	Galloylshikimic acid	Cyclitol phenolic acid
L13	164.0719	1.52	260	$C_9H_{10}NO_2$	+1.3	-	Phenylalanine	Amino acid
L14	305.0669	1.55	260, 369	$C_{15}H_{14}O_7$	+0.7	**125**, 261	Epigallocatechin*	Flavanol
L15	153.0195	1.98	264	$C_7H_6O_4$	+1.4	**109**	Protocatechuic acid*	Phenolic acid
L16	483.0789	2.71	268, 346	$C_{20}H_{20}O_{14}$	+1.7	169, 193, 211, 241, 271, 287, 313, 331, 423, **439**	Gallic acid-galloyl *O*-hexoside isomer	Gallotannin
L17	785.0848	2.71	268, 400	$C_{34}H_{26}O_{22}$	+0.6	275, **300.9**, 419, 483, 633	HHDP digalloyl *O*-hexoside isomer	Ellagitannin
L18	337.0928	3.31	298, 369	$C_{16}H_{18}O_8$	-0.2	119, 155, **163**, 173, 191	Coumaroylquinic acid isomer	Cyclitol phenolic acid
L19	289.0717	3.33	298, 369	$C_{15}H_{14}O_6$	-0.1	125, 135, 167, 179, 205, 231, **245**	Catechin*	Flavanol
L20	183.0300	3.69	258, 370	$C_8H_8O_5$	+0.5	**125**, 151, 168	Methyl gallic acid*	Phenolic acid
L21	353.0881	4.10	248, 292, 323	$C_{16}H_{18}O_9$	+0.8	161, 173, 179, 191, **233**	Chlorogenic acid*	Cyclitol phenolic acid
L22	289.0713	4.38	264, 369	$C_{15}H_{14}O_6$	+1.5	125, 135, 167, 179, 205, 231, **245**	Epicatechin*	Flavanol
L23	483.0786	4.65	264, 370	$C_{20}H_{20}O_{14}$	+1.1	169, 193, 211, 241, 271, 287, 313, 331, 423, **439**	Gallic acid-galloyl *O*-hexoside isomer	Gallotannin
L24	179.0351	5.24	259, 370	$C_9H_8O_4$	+1.1	**109**, 135	Caffeic acid*	Phenolic acid
L25	785.0833	6.16	268, 400	$C_{34}H_{26}O_{22}$	-1.2	275, **300.9**, 419, 483, 633	HHDP digalloyl *O*-hexoside isomer	Ellagitannin
L26	337.0932	8.71	298, 369	$C_{16}H_{18}O_8$	+0.9	119, 137, 163, 173, **191**	Coumaroylquinic acid isomer	Cyclitol phenolic acid
L27	635.0892	9.05	265, 370	$C_{27}H_{24}O_{18}$	+0.4	295, 313, 423, 447, **465**, 483, 617	Trigalloyl *O*-hexoside	Gallotannin
L28	463.0519	9.23	254, 350	$C_{20}H_{16}O_{13}$	+0.3	**300.9**, 447	Ellagic acid *O*-hexoside	Ellagitannin
L29	163.0402	9.39	266, 369	$C_9H_8O_3$	+0.6	**119**, 147	*p*-coumaric acid*	Phenolic acid
L30	367.1035	9.75	272, 369	$C_{17}H_{20}O_9$	+0.2	137, 145, 159, 169, 171, 187, **193**, 221,	Feruloylquinic acid	Cyclitol phenolic acid

						235, 249, 277, 309, 333, 351		
L31	493.0621	10.01	268, 369	$C_{27}H_{18}O_{14}$	-0.6	178.9, 193, 271, 287, 299, **317**, 331, 359, 389, 449, 475	Myricetin 3-*O*-glucuronide	Flavonol
L32	433.0414	10.29	272, 369	$C_{19}H_{14}O_{12}$	+0.4	143, 161, **300.9**, 313, 343, 373, 415	Ellagic acid *O*-pentoside	Ellagitannin
L33	381.1195	10.36	272, 350, 379	$C_{18}H_{22}O_{9}$	+1.0	149, 179, 219, 233, 243, 247, **261**, 273, 291, 333	Ethyl-*O*-caffeoylquinic acid	Cyclitol phenolic acid
L34	615.0992	10.37	272, 350, 379	$C_{28}H_{24}O_{16}$	+0.1	178.9, 211, 241, 255, 271, 283, **301**, 313, 331, 343, 445, 453, 463, 489	Quercetin galloyl *O*-hexoside	Flavonol
L35	300.9991	10.43	254, 369	$C_{14}H_{6}O_{8}$	+0.5	185, 229, **257**, 283	Ellagic acid*	Phenolic acid
L36	787.0996	10.48	268, 350, 378	$C_{34}H_{28}O_{22}$	-0.4	300.9, 403, 447, 449, 465, 483, 573, **617**, 625, 633, 635	Tetragalloyl *O*-hexoside	Gallotannin
L37	609.1459	10.75	285, 382	$C_{27}H_{30}O_{16}$	-0.4	178.9, 255, 271, 285, 297, **301**, 313, 343, 373, 447, 463, 591	Rutin*	Flavonol
L38	477.0677	10.77	277, 345, 384	$C_{21}H_{18}O_{13}$	+0.5	151, 175, 178.9, **301**, 312, 313	Quercetin 3-*O*-glucuronide	Flavonol
L39	463.0883	10.82	259, 353	$C_{21}H_{20}O_{12}$	+0.1	151, 178.9, 255, 271, 273, 287, **301**, 313, 343, 445	Quercetin 3-*O*-glucoside*	Flavonol
L40	593.1514	11.11	269, 369	$C_{27}H_{30}O_{15}$	+0.4	187, 197, 213, 229, 241, 255, 267, **285**, 309, 327, 357, 358, 369, 393, 429, 447, 533, 565	Kaempferol 3-*O*-rutinoside	Flavonol
L41	433.0776	11.12	269, 369	$C_{20}H_{18}O_{11}$	-0.1	151, 255, **301**	Quercetin *O*-pentoside isomer	Flavonol
L42	395.1350	11.20	267, 350, 423	$C_{19}H_{24}O_{9}$	+0.7	217, 233, 247, 257, 263, **275**, 305, 317, 329, 341, 359, 377	Unknown	Unknown
L43	483.1874	11.27	258, 369	$C_{23}H_{32}O_{11}$	+0.4	151, **169**, 181, 209, 211, 223, 253, 271, 313, 439	Globulusin A	Gallotannin monoterpene
L44	461.0727	11.29	286, 327, 348, 383	$C_{21}H_{18}O_{12}$	+0.3	157, 175, 197, 229, 241, 257, 267, **285**, 295, 315, 327, 443	Kaempferol *O*-glucuronide	Flavonol
L45	447.0935	11.35	266, 346	$C_{21}H_{20}O_{11}$	+0.6	151, 178.9, 227, 255, **301**, 315, 321, 327, 343, 357, 429	Quercitrin	Flavonol
L46	585.0889	11.42	296, 382	$C_{27}H_{22}O_{15}$	+0.5	255, 273, 283, **301**, 433, 453	Quercetin galloyl *O*-pentoside	Flavonol
L47	417.0828	11.49	282, 345, 382	$C_{20}H_{18}O_{10}$	+0.2	151, 227, 255, 257, 269, 283, **285**, 327, 357, 389	Kaempferol *O*-arabinoside	Flavonol
L48	445.0777	11.57	273, 343, 435	$C_{21}H_{18}O_{11}$	+0.2	129, 157, 175, **269**, 311, 341, 427	Apigenin *O*-glucuronide	Flavone
L49	431.0988	11.89	268, 338, 369	$C_{21}H_{20}O_{10}$	+0.9	151, **269**, 283, 311, 341, 371, 413	Apigenin 7-*O*-glucoside*	Flavone
L50	315.0149	11.63	268, 336	$C_{15}H_{8}O_{8}$	+0.8	**300.9**	3-methylellagic acid	Phenolic acid
L51	435.1302	11.70	268, 336	$C_{21}H_{24}O_{10}$	+1.1	167, 179, **273**, 297, 315	Phlorizin*	Dihydrochalcone

L52	629.1880	12.44	290, 343, 381	$C_{31}H_{34}O_{14}$	+0.7	178.9, 255, 271, 273, **301**, 343, 445, 463, 571, 581, 611	Quercetin (oleuropeoyl) *O*-hexoside	Flavonol
L53	267.1241	12.54	265, 338, 369	$C_{14}H_{20}O_5$	+1.1	99, 113, 125, 141, 165, 179, 181, 197, 205, **223**, 225, 249	Endoperoxide G3	Endoperoxide
L54	287.0565	12.54	358	$C_{15}H_{12}O_6$	+1.5	135, **151**, 169, 217	Eriodyctiol*	Flavanone
L55	317.0307	12.62	269, 354	$C_{15}H_{10}O_8$	+1.3	**299**, 193, 151	Myricetin*	Flavonol
L56	301.0355	12.62	269, 354	$C_{15}H_{10}O_7$	+0.4	273, 257, **178.9**, 151, 125	Quercetin*	Flavonol
L57	285.0406	12.62	299, 385	$C_{15}H_{10}O_6$	+0.6	133, **151**, 175	Luteolin*	Flavone
L58	181.0144	12.64	268, 336, 470	$C_8H_6O_5$	+1.0	89, 102, 111, 122, 125, 135, 137, **153**	Diformylphloroglucinol	FPC
L59	613.1929	12.75	272, 361	$C_{31}H_{34}O_{13}$	+0.3	187, 211, 229, 255, **285**, 447, 493, 585, 595	Kaempferol (oleuropeoyl) *O*-hexoside	Flavonol
L60	273.0763	13.21	272, 350	$C_{15}H_{14}O_5$	-1.9	123, **125**, 167, 179	Phloretin*	Dihydrochalcone
L61	269.0458	13.37	269, 336, 369	$C_{15}H_{10}O_5$	+1.1	117, 149, 159, 183, 201, **225**	Apigenin*	Flavone
L62	271.0614	13.37	269, 336, 369	$C_{15}H_{12}O_5$	+0.8	107, 119, 125, **151**, 165	Naringenin*	Flavanone
L63	285.0407	13.50	231, 267, 360	$C_{15}H_{10}O_6$	+0.8	135, **151**, 187	Kaempferol*	Flavonol
L64	327.2181	13.72	-	$C_{18}H_{32}O_5$	+1.2	99, 139, 157, 171, 211, **229**, 293, 311	9,12,13-trihydroxy-10,15-octadecadienoic acid	Fatty acid
L65	577.1353	13.89	270, 327, 399	$C_{30}H_{26}O_{12}$	+0.2	245, 273, 289, 299, 331, 381, 407, **425**, 433, 451	B type proanthocyanidin	Flavanol
L66	329.2339	14.19	-	$C_{18}H_{34}O_5$	+1.8	125, 139, 155, 183, 197, 201, 209, 211, **229**, 291	9,12,13-trihydroxy-10-octadecenoic acid	Fatty acid
L67	223.0979	14.98	273, 327, 369	$C_{12}H_{16}O_4$	+1.4	85, 99, 111, 123, 137, 153, 161, 167, **179**, 182, 196, 205, 208	2,6-dihydroxy-4-methoxy-3-methylisopropiophenone	Phloroglucinol
L68	265.0722	14.98	273, 327, 369	$C_{13}H_{14}O_6$	+1.6	111, 125, 151, 167, 191, **195**, 209, 221, 237, 247	Jensenone	FPC
L69	209.0823	15.27	223, 288, 368	$C_{11}H_{14}O_4$	+1.8	125, 139, 152,166, 181, 191, **194**	Robustaol B	Phloroglucinol
L70	253.1079	15.50	273, 325	$C_{13}H_{18}O_5$	+0.7	83, 99, 109, 127, 165, 169, 181, 191, 193, 197, 209, 211, 225, **235**	Unknown FPC	FPC
L71	237.1133	15.75	231, 287, 337	$C_{13}H_{18}O_4$	+0.4	85, 97, 111, 125, 137, 153, 164, 179, **193**, 219	Phloroglucinol derivative	Phloroglucinol
L72	313.2386	16.03	-	$C_{18}H_{34}O_4$	+0.5	-	Dihydroxy octadecenoic acid	Fatty acid
L73	419.1352	16.04	223, 276	$C_{21}H_{24}O_9$	+1.0	125, 169, 181, 197, 209, 223, 235, **237**, 249, 253, 375	Unknown FPC	FPC
L74	297.0773	16.44	280, 320	$C_{17}H_{14}O_5$	+1.6	119, 121, 145, 163, 181 239 255, 267, **282**, 284	8-desmethylsideroxylin	Flavone
L75	311.0930	16.77	281, 326	$C_{18}H_{16}O_5$	+1.5	225, 267, 280, 281, **296**	8-Demethyleucalyptin*	Flavone

L76	721.3657	16.98		$C_{34}H_{58}O_{16}$	+0.6	235, 277, 287, 305, 323, 397, 415, 493, 526, **675**	Sesquiterpene alcohol bis FPC	FPC
L77	251.1288	17.12	224, 277, 327	$C_{14}H_{20}O_4$	-0.5	123, 125, 127, 137, 149, 150, 164, 167, 193, **207**, 233	Phloroglucinol derivative	Phloroglucinol
L78	293.2126	17.33	-	$C_{18}H_{30}O_3$	+1.4	-	Hydroxy octadecatrienoic acid	Fatty acid
L79	267.0879	17.38	231, 285, 336	$C_{13}H_{16}O_6$	+1.9	141, 183, 197, 223, 225, **249**	Unknown FPC	FPC
L80	251.0925	17.74	280, 336	$C_{13}H_{15}O_5$	+0.1	97, 125, 167, 207, **223**, 233	Grandinol	FPC
L81	403.1405	18.08	270	$C_{21}H_{24}O_8$	+1.6	165, 209, 235, **237**, 250	Unknown FPC	FPC
L82	471.1666	18.19	272, 320, 341	$C_{25}H_{28}O_9$	+1.2	181, 237, 249, **251**, 418, 391, 445	Unknown FPC	FPC
L83	503.1924	18.24	231, 291, 330	$C_{26}H_{32}O_{10}$	+0.2	191, 193, 197, 207, 209, 211, 221, 235, 237, 247, 249, **253**, 305, 443, 459, 485	Unknown FPC	FPC
L84	265.1085	18.43	224, 280, 358	$C_{14}H_{18}O_5$	+1.2	183, 197, 205, 223, 237, **249**	Homograndinol	FPC
L85	277.2174	18.43	-	$C_{18}H_{30}O_2$	+0.4	-	Linolenic acid	Fatty acid
L86	485.1819	18.48	277, 326, 349	$C_{26}H_{30}O_9$	+0.4	151, 181, 193, 207, 223, 235, **249**, 291, 317, 439	Dimer of grandinol	FPC
L87	403.2130	18.81	277, 326, 349	$C_{23}H_{32}O_6$	+0.8	165, 181, 193, **207**, 221, 237, 249, 250, 287, 311, 317, 331, 346, 359, 375, 385	Monoterpene alcohol FPC	FPC
L88	417.1192	18.83	277, 326, 349	$C_{21}H_{22}O_9$	+0.2	123, 139, 151, 165, 167, 179, 209, 235, **237**, 249, 319, 389	Unknown FPC	FPC
L89	279.2330	19.02	-	$C_{18}H_{32}O_2$	+0.2	-	Linoleic acid	Fatty acid
L90	255.2329	19.84	-	$C_{16}H_{31}O_2$	+0.3	-	Palmitic acid	Fatty acid
L91	471.2753	20.03	225, 272, 366	$C_{28}H_{40}O_6$	+0.3	165, 181, 193, **207**, 221, 235, 250, 291, 302, 305, 355, 369, 385, 397, 411, 413, 443, 453	Macrocarpal type FPC	FPC
L92	281.2486	20.04	-	$C_{18}H_{34}O_2$	0.0	-	Stearic acid	Fatty acid
L93	487.1614	20.15	225, 277, 327, 376	$C_{25}H_{28}O_{10}$	+0.9	153, 181, 193, 193, 209, 219, **237**, 249, 305, 320, 385	Dimer of grandinol	FPC
L94	473.1814	20.22	275, 316	$C_{25}H_{30}O_9$	-0.6	153, 181, 207, 223, 237, **249**, 291	Jensenal	FPC
L95	459.1662	20.40	270, 320	$C_{24}H_{28}O_9$	+0.3	135, 151, 165, 178, 181, 193, 209, 221, 235, **237**, 249, 250	Unknown FPC	FPC
L96	499.1613	20.64	230, 280, 340	$C_{26}H_{28}O_{10}$	+0.7	165, 179, 181, 193, 219, 221, 237, **249**, 261, 305, 317, 471	Grandinal	FPC
L97	385.2024	21.55	232, 287, 322	$C_{23}H_{30}O_5$	+0.9	165, 177, 181, 193, 205, **207**, 219, 221, 233, 259, 269, 285, 313, 317, 328, 357	Euglobal type FPC	FPC

* Confirmed with authentic standards. Product ions in bold are the base peaks of the MS/MS spectra.

Table 2. ^{1}H and ^{13}C NMR data and key ^{1}H-^{13}C HMBC correlations of metabolites identified in eucalypt leaf extract (CD_3OD, 400 MHz for ^{1}H and 150 MHz for ^{13}C).

No.	Metabolite	Position	δ ^{1}H [ppm][a] Mult. (J [Hz])	δ ^{13}C shift [ppm][b]	HMBC (H to C)
N1	Fatty acids	1	-	174.7	
		2	2.325 *t* (7.8)	35.0	1
		ω	0.89	14.5	ω-1, ω-2
		ω-2	1.28	32.8	
		ω-1	1.31	23.8	
N2	Linolenic acid	9/10/12/13/15/16	5.32-5.39	129.1, 130.9	11/14
		11/14	2.808 *t* (6.0)	26.4	9/10/12/13/15/16
		4/5/6/7	1.327	29.4	
		18	0.971 *t* (7.5)	14.6	
N3	α-glucose	1	5.105 *d* (3.7)	94.0	
N4	β-glucose	1	4.472 *d* (7.8)	98.2	
N5	*myo*-inositol	1	3.958 *t* (2.7)	74.1	
		2	3.463	74.9	
		4	3.145 *t* (9.2)	75.6	
N6	Shikimic acid	1	-	170.1	
		3	6.794 *m*	138.7	1, 5, 7
		4	4.371 *m*	67.3	3, 6
		5	3.67	72.7	
		6	3.99	68.4	
		7a	2.193 *dd* (18.0, 5.0)	31.7	1, 3
		7b	2.698 *dd* (18.0, 5.0)	31.7	1, 3
N7	Gallic acid	1	-	170.3	
		2	-	121.8	
		3/7	7.056 *s*	110.2	1, 2, 4/6, 5
		4/6	-	146.3	
		5	-	139.5	
N8	Kaempferol 3-*O*-substituted	6	6.185 *d* (2.0)	99.9	8
		8	6.401 *d* (2.0)	94.7	6
		2′/6′	8.08 *d* (8.8)	132.2	3, 4′, 3′/5′
		4′	-	161.52	
		3′/5′	6.90 *d* (8.8)	116.2	4′
N9	Quercetin 3-*O*-substituted	6	6.185 *d* (2.0)	99.9	8
		8	6.401 *d* (2.0)	94.7	6
		5′	6.88	116.0	6′
		6′	7.568 *dd* (8.0, 2.0)	123.1	5′
N10	Arginine	4	1.60 m	26.0	3
		3	2.00 m	28.2	

s singlet; *d* doublet; *t* triplet; *dd* doublet of doublet; *m* multiplet. [a] ^{1}H chemical shifts with only two decimal places are chemical shifts of HSQC correlation peaks or signal overlapping [b] Chemical shifts of HSQC or HMBC correlation peaks.

Table 3. Metabolite content expressed as mg g^{-1} leaf dry weight in eucalypt seedlings grown at well-watered (WW) and water-deficit (WD) conditions. Results were obtained by ^{1}H-NMR analysis of extracts in CD_3OD.

Clone	Response to drought	Growth condition	Glucose	Inositol	Shikimic acid	Arginine
Suz1	Sensitive	WW	**12.13 ± 2.7**	**16.42 ± 3.8**	**4.24 ± 1.3**	29.28 ± 12.3
		WD	**3.19 ± 0.8**	**7.38 ± 1.2**	**1.61 ± 0.5**	31.28 ± 2.4

Suz2	Sensitive	WW	**29.88 ± 11.7**	**12.68 ± 1.8**	**9.23 ± 2.4**	**27.85 ± 10.8**
		WD	**10.57 ± 2.5**	**18.06 ± 2.5**	**5.02 ± 0.1**	**50.94 ± 7.2**
Suz3	Sensitive	WW	**14.77 ± 2.3**	**24.67 ± 7.0**	**13.96 ± 0.4**	**64.96 ± 3.6**
		WD	**5.43 ± 0.9**	**11.39 ± 2.2**	**5.6 ± 0.9**	**44.02 ± 5.4**
Suz7	Sensitive	WW	**5.2 ± 0.9**	10.89 ± 2.8	**7.35 ± 2.8**	31.97 ± 5.5
		WD	**3.1 ± 0.3**	7.19 ± 1.1	**3.28 ± 0.1**	41.85 ± 8.4
Suz13	Sensitive	WW	**6.2 ± 0.4**	**9.26 ± 0.9**	**6.36 ± 1.0**	50.82 ± 7.6
		WD	**12.48 ± 1.0**	**15.47 ± 3.1**	**3.6 ± 1.1**	43.66 ± 9.0
Suz4	Tolerant	WW	**6.81 ± 1.3**	**14.07 ± 2.3**	**5.07 ± 0.4**	52.44 ± 8.5
		WD	**12.49 ± 1.9**	**18.32 ± 2.8**	**9.12 ± 1.5**	43.62 ± 2.5
Suz5	Tolerant	WW	**8.1 ± 1.2**	**13.95 ± 2.3**	**8.05 ± 0.8**	**34.44 ± 7.5**
		WD	**3.69 ± 0.8**	**8.43 ± 1.4**	**4.53 ± 0.8**	**47.04 ± 5.2**
Suz6	Tolerant	WW	**10.53 ± 0.9**	13.3 ± 1.3	**5.29 ± 0.2**	**49.77 ± 5.9**
		WD	**7.1 ± 1.3**	13.31 ± 0.7	**3.07 ± 0.4**	**61.33 ± 6.5**
Suz8	Tolerant	WW	14.47 ± 2.8	**14.66 ± 2.4**	9.27 ± 3.7	**25.3 ± 5.4**
		WD	14.12 ± 4.3	**26.11 ± 7.2**	8.34 ± 4.6	**41.41 ± 4.3**
Suz9	Tolerant	WW	9.93 ± 0.8	11.67 ± 2.2	2.96 ± 0.8	**64.15 ± 12.1**
		WD	9.39 ± 0.6	12.39 ± 2.1	3.31 ± 1.2	**48.09 ± 7.5**
Suz11	Tolerant	WW	**4.11 ± 0.3**	10.63 ± 0.5	5.03 ± 1.5	**29.62 ± 5.0**
		WD	**5.93 ± 0.7**	11.37 ± 1.3	4.35 ± 0.9	**57.6 ± 8.5**
Suz12	Tolerant	WW	10.66 ± 0.9	**13 ± 1.2**	5.19 ± 0.1	**24.98 ± 5.1**
		WD	10.78 ± 3.7	**17.86 ± 1.5**	4.17 ± 1.7	**56.19 ± 14.3**

Quantitation was carried out relative to the internal standard hexamethyldisiloxane, 0.94 mM. Values are the mean ± SE of measurements made on biological and technical replicates. Data in bold indicate WW and WD samples of the same clone that were statistically different ($P < 0.05$, Tukey's post-test). In gray the ones that are not different.

Table 4. Commercial clones of *Eucalyptus* spp. and their response to drought (data provided by Suzano S/A, based on the clones' response in the field).

Clones	**Genetic background**	**Response to drought**
Suz1	*Eucalyptus grandis* × *urophylla*	Sensitive
Suz2	*Eucalyptus grandis* × *urophylla*	Sensitive
Suz3	*Eucalyptus grandis* × *urophylla*	Sensitive
Suz4	*Eucalyptus platyphylla*	Tolerant
Suz5	*Eucalyptus grandis* × *pellita*	Tolerant
Suz6	*Eucalyptus grandis* × *urophylla*	Tolerant
Suz7	*Eucalyptus grandis* × *pellita*	Sensitive
Suz8	*Eucalyptus grandis*	Tolerant
Suz9	*Eucalyptus urophylla*	Tolerant
Suz10	*Eucalyptus grandis*	Sensitive
Suz11	*Eucalyptus grandis* × *urophylla*	Tolerant
Suz12	*Eucalyptus. grandis* × *urophylla*	Tolerant
Suz13	*Eucalyptus grandis* × *urophylla*	Sensitive